

MICROCOPY RESOLUTION TEST CHART
NATIONAL BUREAU OF STANDARDS 1963-A

AD-A184 902

DTIC FILE COPY

2

NAVAL POSTGRADUATE SCHOOL

Monterey, California



THESIS

INVESTIGATION BY DIFFERENTIAL SCANNING
CALORIMETRY OF MICROSTRUCTURE IN A
SUPERPLASTIC Al-Mg-Zr ALLOY

by

Donald L. Stewart, II

June 1987

Thesis Advisor:

T.R. McNelley

Approved for public release; distribution is unlimited

DTIC

OCT 14 1987

ck

H

87 9 29 122

UNCLASSIFIED

SECURITY CLASSIFICATION OF THIS PAGE

ADA184902

REPORT DOCUMENTATION PAGE

1a REPORT SECURITY CLASSIFICATION UNCLASSIFIED		1b RESTRICTIVE MARKINGS	
2a SECURITY CLASSIFICATION AUTHORITY		3 DISTRIBUTION/AVAILABILITY OF REPORT Approved for public release; distribution is unlimited	
2b DECLASSIFICATION/DOWNGRADING SCHEDULE		5 MONITORING ORGANIZATION REPORT NUMBER(S)	
4 PERFORMING ORGANIZATION REPORT NUMBER(S)		7a NAME OF MONITORING ORGANIZATION Naval Postgraduate School	
6a NAME OF PERFORMING ORGANIZATION Naval Postgraduate School	6b OFFICE SYMBOL (if applicable) Code 54	7b ADDRESS (City, State, and ZIP Code) Monterey, California 93943-5000	
6c ADDRESS (City, State, and ZIP Code) Monterey, California 93943-5000		9 PROCUREMENT INSTRUMENT IDENTIFICATION NUMBER	
8a NAME OF FUNDING/SPONSORING ORGANIZATION	8b OFFICE SYMBOL (if applicable)	10 SOURCE OF FUNDING NUMBERS	
8c ADDRESS (City, State, and ZIP Code)		PROGRAM ELEMENT NO	PROJECT NO
		TASK NO	WORK UNIT ACCESSION NO
11 TITLE (Include Security Classification) INVESTIGATION BY DIFFERENTIAL SCANNING CALORIMETRY OF MICROSTRUCTURE IN A SUPERPLASTIC Al-Mg-Zr ALLOY			
12 PERSONAL AUTHOR(S) Stewart, Donald L. II			
13 TYPE OF REPORT Master's Thesis	13b TIME COVERED FROM TO	14 DATE OF REPORT (Year, Month, Day) 1987, June	15 PAGE COUNT 92
6 SUPPLEMENTARY NOTATION			
COSAT CODES		18 SUBJECT TERMS (Continue on reverse if necessary and identify by block number)	
FIELD	GROUP	SUB-GROUP	
		Superplasticity; Aluminum Alloys; Thermomechanical Processing; Differential Scanning Calorimetry	
7 ABSTRACT (Continue on reverse if necessary and identify by block number) The three significant variables identified in thermomechanical processing of an Al-10Mg-0.1Zr alloy to obtain superplastic ductilities are reduction per pass, reheating time between passes, and total strain during warm rolling at 573K. The effect of adjusting these variables on elevated temperature mechanical properties has been evaluated and the microstructures characterized using transmission electron microscopy. Comparison of the differential scanning calorimetry results with mechanical property and microstructural data reveal that the endothermic energy absorbed by the material, which is related to microstructural stability, can be correlated with superplastic behavior.			
20 DISTRIBUTION/AVAILABILITY OF ABSTRACT <input checked="" type="checkbox"/> UNCLASSIFIED/UNLIMITED <input type="checkbox"/> SAME AS RPT <input type="checkbox"/> DTIC USERS		21 ABSTRACT SECURITY CLASSIFICATION Unclassified	
22a NAME OF RESPONSIBLE INDIVIDUAL Professor T.R. McNelley		22b TELEPHONE (Include Area Code) (408) 646-2589	22c OFFICE SYMBOL Code 69Mc

Approved for public release; distribution is unlimited

Investigation by Differential Scanning Calorimetry of
Microstructure in a Superplastic Al-Mg-Zr Alloy

by

Donald L. Stewart, II
Lieutenant Commander, United States Navy
B.S., U.S. Naval Academy 1977

Submitted in partial fulfillment of the
requirements for the degrees of

MASTER OF SCIENCE IN MECHANICAL ENGINEERING

and

MECHANICAL ENGINEER

from the

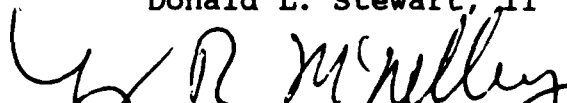
NAVAL POSTGRADUATE SCHOOL
June 1987

Author:

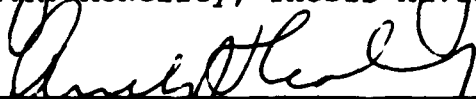


Donald L. Stewart, II


Approved by:



T.R. McNelley, Thesis Advisor



Anthony J. Healey, Chairman
Department of Mechanical Engineering



Gordon E. Schacher
Dean of Science and Engineering

ABSTRACT

The three significant variables identified in thermo-mechanical processing of an Al-10Mg-0.1Zr alloy to obtain superplastic ductilities are reduction per pass, reheating time between passes, and total strain during warm rolling at 573K. The effect of adjusting these variables on elevated temperature mechanical properties has been evaluated and the microstructures characterized using transmission electron microscopy. Comparison of the differential scanning calorimetry results with mechanical property and microstructural data reveal that the endothermic energy absorbed by the material, which is related to microstructural stability, can be correlated with superplastic behavior.



Accession For	
NTIS GRA&I	<input checked="" type="checkbox"/>
DTIC TAB	<input type="checkbox"/>
Unannounced	<input type="checkbox"/>
Justification	
By	
Date	

A-1

TABLE OF CONTENTS

I.	INTRODUCTION -----	11
II.	BACKGROUND -----	13
	A. ALUMINUM ALLOYS--GENERAL -----	13
	B. ALLOYING ELEMENTS -----	14
	C. SUPERPLASTICITY -----	14
	D. DIFFERENTIAL SCANNING CALORIMETRY -----	17
	E. TRANSMISSION ELECTRON MICROSCOPY -----	19
	F. SUMMARY -----	19
III.	EXPERIMENTAL PROCEDURE -----	20
	A. MATERIAL -----	20
	B. THERMOMECHANICAL PROCESSING -----	20
	C. SAMPLE PREPARATION -----	22
	D. MEASUREMENTS AND DATA REDUCTION -----	22
	1. Tensile Testing -----	22
	2. Calorimetry -----	23
	E. MICROSCOPY -----	24
IV.	RESULTS AND DISCUSSION -----	25
	A. MECHANICAL PROPERTIES -----	25
	1. Effect of Total Rolling Strain (1.5 vs. 2.5) -----	27
	2. Effect of Reheating Time Between Passes (4 vs. 30 Min) -----	30
	3. Effect of Reduction Per Pass (1 mm vs. 2.5 mm) -----	33
	4. Summary -----	36

B.	DIFFERENTIAL SCANNING CALORIMETRY -----	38
1.	Effect of Total Rolling Strain (1.5 vs. 2.5) -----	40
2.	Effect of Reduction Per Pass (1 mm vs. 2.5 mm) -----	43
3.	Effect of Reheating Time Between Passes (4 Min vs. 30 Min) -----	53
4.	Summary -----	53
C.	TRANSMISSION ELECTRON MICROSCOPY -----	56
1.	As-rolled Microstructure -----	57
2.	Microstructure After 10 Hour Anneal at 573K (300°C) -----	59
3.	Comparison of As-rolled and the 10 hour Anneal Samples -----	65
4.	TMP2 and TMP6: Annealed One Hour -----	65
5.	Grip Section Microstructure -----	68
V.	CONCLUSIONS AND RECOMMENDATIONS -----	71
A.	CONCLUSIONS -----	71
B.	RECOMMENDATIONS -----	72
APPENDIX A:	COMPUTER PROGRAM -----	74
APPENDIX B:	STRESS VS. STRAIN GRAPHS -----	75
APPENDIX C:	HEAT CAPACITY VS. TEMPERATURE GRAPHS OF DSC DATA -----	80
LIST OF REFERENCES	-----	86
INITIAL DISTRIBUTION LIST	-----	90

LIST OF TABLES

I.	ALLOY COMPOSITION (WEIGHT PERCENT) -----	20
II.	THERMOMECHANICAL PROCESSING SCHEDULES -----	21
III.	HEAT TREATMENT SCHEDULES FOR TMP2 AND TMP3 -----	46

LIST OF FIGURES

2.1	Differential Scanning Calorimeter Schematic -----	18
4.1	True Stress vs. True Strain Plot for Tensile Testing Conducted at 300°C for an Al-10Mg-0.1Zr Alloy. The Specimen was Heat Treated and Upset Forged as Described in This Work and Warm Rolled Using Schedule TMP2 Described in Table II -----	26
4.2	Graph of (a) Percent Elongation vs. Log Strain Rate and (b) Log True Stress vs. Log Strain Rate for TMP2 and TMP5 -----	28
4.3	Graph of (a) Percent Elongation vs. Log Strain Rate and (b) Log True Stress vs. Log Strain Rate for TMP3 and TMP4 -----	29
4.4	Graph of (a) Percent Elongation vs. Log Strain Rate and (b) Log True Stress vs. Log Strain Rate for TMP1 and TMP3 -----	31
4.5	Graph of (a) Percent Elongation vs. Log Strain Rate and (b) Log True Stress vs. Log Strain Rate for TMP2 and TMP6 -----	32
4.6	Graph of (a) Percent Elongation vs. Log Strain Rate and (b) Log True Stress vs. Log Strain Rate for TMP2 and TMP3 -----	34
4.7	Graph of (a) Percent Elongation vs. Log Strain Rate and (b) Log True Stress vs. Log Strain Rate for TMP1 and TMP6 -----	35
4.8	Partial Aluminum-Magnesium Phase Diagram with TMP Region Indicated -----	40
4.9	Graph of Heat Capacity vs. Temperature for Processes TMP3 and TMP4 -----	42
4.10	Graph of Heat Capacity vs. Temperature for Processes TMP2 and TMP3 -----	44
4.11	Graph of Heat Capacity vs. Temperature for Processes T200, T240, T300 and T340 -----	47

4.12	Graph of Heat Capacity vs. Temperature for Processes TMP2, T200 and T240 -----	48
4.13	Graph of Heat Capacity vs. Temperature for Processes TMP3, T300 and T340 -----	49
4.14	Graph of Heat Capacity vs. Temperature for Processes TMP6 and TMP1 -----	51
4.15	Graph of Heat Capacity vs. Temperature for Processes TMP2 and TMP6 -----	54
4.16	Graph of Heat Capacity vs. Temperature for Processes TMP1 and TMP3 -----	55
4.17	TEM Micrograph of an Al-10Mg-0.1Zr Alloy in the As-rolled Condition (a) TMP2 (b) TMP6 ----	58
4.18	TEM Micrograph of an Al-10Mg-0.1Zr Alloy in the 10 Hour Annealed Condition (a) TMP2 (b) TMP6 -----	60
4.19	TEM Micrograph of an Al-10Mg-0.1Zr Alloy Processed by TMP2 and Annealed for 10 Hours (a) Bright Field (b) Dark Field -----	61
4.20	TEM Micrograph of an Al-10Mg-0.1Zr Alloy Processed by TMP6 and Annealed for 10 Hours (a) Bright Field (b) Dark Field -----	63
4.21	TEM Micrograph of an Al-10Mg-0.1Zr Alloy Processed by TMP6 and Annealed for 10 Hours (a) Bright Field (b) Dark Field -----	64
4.22	TEM Micrograph of an Al-10Mg-0.1Zr Alloy in the 1 Hour Annealed Condition (a) TMP2 (b) TMP6 -----	66
4.23	TEM Micrograph of an Al-10Mg-0.1Zr Alloy Processed by TMP2 and Annealed for 42 Hours ----	67
4.24	TEM Micrograph of an Al-10Mg-0.1Zr from the Grip Section of a Tensile Test Sample (a) TMP2 (b) TMP6 -----	69
B.1	True Stress vs. True Strain Plot for Tensile Testing Conducted at 300°C for an Al-10Mg- 0.1Zr Alloy. The Specimen was Heat Treated and Upset Forged as Described in This Work and Warm Rolled Using Schedule TMP1 Described in Table II -----	75

B.2	True Stress vs. True Strain Plot for Tensile Testing Conducted at 300°C for an Al-10Mg-0.1Zr Alloy. The Specimen was Heat Treated and Upset Forged as Described in This Work and Warm Rolled Using Schedule TMP3 Described in Table II -----	76
B.3	True Stress vs. True Strain Plot for Tensile Testing Conducted at 300°C for an Al-10Mg-0.1Zr Alloy. The Specimen was Heat Treated and Upset Forged as Described in This Work and Warm Rolled Using Schedule TMP4 Described in Table II -----	77
B.4	True Stress vs. True Strain Plot for Tensile Testing Conducted at 300°C for an Al-10Mg-0.1Zr Alloy. The Specimen was Heat Treated and Upset Forged as Described in This Work and Warm Rolled Using Schedule TMP5 Described in Table II -----	78
B.5	True Stress vs. True Strain Plot for Tensile Testing Conducted at 300°C for an Al-10Mg-0.1Zr Alloy. The Specimen was Heat Treated and Upset Forged as Described in This Work and Warm Rolled Using Schedule TMP6 Described in Table II -----	79
C.1	Plot of Heat Capacity vs. Temperature, Raw Data, for Each of the Three DSC Runs, Plus the Average for TMP1 -----	80
C.2	Plot of Heat Capacity vs. Temperature, Raw Data, for Each of the Three DSC Runs, Plus the Average for TMP2 -----	81
C.3	Plot of Heat Capacity vs. Temperature, Raw Data, for Each of the Three DSC Runs, Plus the Average for TMP3 -----	82
C.4	Plot of Heat Capacity vs. Temperature, Raw Data, for Each of the Three DSC Runs, Plus the Average for TMP4 -----	83
C.5	Plot of Heat Capacity vs. Temperature, Raw Data, for Each of the Three DSC Runs, Plus the Average for TMP6 -----	84
C.6	Average Heat Capacity vs. Temperature Plots for All TMPs Investigated by DSC -----	85

ACKNOWLEDGEMENTS

I would like to thank my advisor, Professor T.R. McNelley for his expert assistance as I conducted this research. Also, I would like to express my sincerest gratitude to Dr. S.J. Hales for the expert, tireless assistance and guidance he provided as my (tor)'mentor' during my research. Also, I want to thank Tammy Bloomer and Tom Kellog for their technical assistance. Without the assistance of Jim Wise and Ahmed Salama during the processing phase of this research, I wouldn't have been able to do a complete job, so thanks to the both of you.

Without the support of loved ones a task like this research is basically impossible. So, I want to thank my bride, Kimberly, for her support, especially during the time of those 'long' days, and my daughter, Joy Louise, for her cheerful attitude that helped make our home a joyful place to return to after the tedious days of work.

I. INTRODUCTION

Superplasticity refers to the ability of a material to elongate more than 200 percent in tension when it is tested under certain combinations of strain rate and temperature. Superplastic elongations of 500 percent are frequently reported and values of elongation in excess of 1000 percent are not uncommon. When it was first reported by Rosenhain in 1920, as noted by Johnson [Ref. 1:p. 115], a cold-rolled zinc-copper-aluminum eutectic alloy exhibited this superplastic response. Superplasticity was initially viewed as a curious observation limited to eutectic alloys when tested under the correct laboratory conditions. However, in 1962 Underwood [Ref. 2] reviewed Soviet work; this review caused the rest of the world to take note and investigation into superplastic response of many materials began in earnest. Interest has continued to increase and in the recent past the commercial applications of superplastic aluminum alloys has redoubled the interest and research into this field.

The commercial applications include the ability to form complex shapes from a single piece of material while maintaining extremely accurate dimensions. Additionally, the complexity and cost of the special tooling for forming these complex shapes has been drastically reduced. The

greatest impact of superplastic forming will be felt in the aerospace industry as the requirements for fasteners and weldments are minimized. Also, while maintaining good mechanical properties the weight of these superplastically formed shapes is less than that of the original component with its associated fasteners.

Research at the Naval Postgraduate School in the recent past has centered on a high-Mg, Al-Mg-Zr alloy. This type of alloy was chosen because it has a relatively high strength, low density and can superplastically deform after being properly processed. The purpose of this thesis is to examine how changing the thermomechanical processing variables affects the superplasticity and to correlate this information with data concerning microstructural evolution and the stability (or lack of stability) of the microstructure as detected by the differential scanning calorimeter and as seen through the transmission electron microscope.

II. BACKGROUND

A. ALUMINUM ALLOYS--GENERAL

Aluminum alloys are widely used industrially and are of special interest for military and aerospace applications due to good strength-to-weight ratios, low density, and good ductility. In general, aluminum alloys are strengthened by solid solution, precipitation, and dispersion strengthening mechanisms.

Solid solution strengthening occurs by a variety of mechanisms reviewed by Meyers and Chawla [Ref. 3:pp. 387-393] and Dieter [Ref. 4:p. 213]. Precipitation strengthening, or age hardening, is designed to impede dislocation motion in a relatively soft, ductile material, like aluminum, by a fine homogeneous dispersion of a hard precipitate throughout the parent metal matrix. The three basic steps to accomplish this, described in detail by Askeland [Ref. 5:p. 281] are:

- 1) Solution treatment
- 2) Quenching
- 3) Aging.

Dispersion strengthening is accomplished, similar to precipitation strengthening, by introducing a second phase into the parent matrix. These disperoids, like the precipitates, are hard particles which restrict dislocation

motion, stabilize dislocation structures and thereby strengthen the parent metal.

B. ALLOYING ELEMENTS

The principal alloying addition in the material of this research is magnesium (Mg), nominally 10 weight percent. Since magnesium is less dense than aluminum, its addition reduces the density of the alloy. The addition of magnesium enhances the alloy's weldability and corrosion resistance [Ref. 6:p. 147] while also providing solid solution strengthening. As reported by Mondolfo [Ref. 7:pp. 311-317] the precipitation sequence is from a supersaturated solution to Al + β (Mg_5Al_8) upon cooling. It is the precipitation of this β phase during processing that has been a focal point of research at NPS.

The second element added, zirconium (Zr), is present in the amount of 0.1 weight percent nominally. This addition results in the formation of a very fine dispersoid, $ZrAl_3$. This dispersoid results in grain refinement, raises the recrystallization temperature [Ref. 7:p. 414] and gives rise to the potential for control of recrystallization during processing [Ref. 8:p. 2320].

C. SUPERPLASTICITY

A complete explanation for superplasticity has not been presented. Consequently, phenomenological models have been proposed, of which the most widely accepted is the Sherby-

Wadsworth model [Ref. 9:p. 242]. This model indicates that the superplastic strain rate is inversely proportional to the microstructure's grain size. Identification of an acceptable model has led to the development of prerequisites of superplastic materials, which are [Refs. 9:p. 245; 10:pp. 3-10; 11:pp. 324-334; 12:pp. 151-152; 13:pp. 367-371]:

- 1) a fine, equiaxed grain size (<10 microns) with boundary misorientation sufficient to support grain boundary sliding
- 2) mobile grain boundaries
- 3) a deformable second phase
- 4) a thermally stable microstructure at the deformation temperature
- 5) a resistance to cavitation
- 6) low strain rates
- 7) elevated temperatures (0.5 to 0.7 T_m).

To attain these conditions requires that a method of grain refinement be identified.

Grain size control is obtained by controlling the effects of recovery, discontinuous recrystallization and continuous recrystallization that may occur upon heating after mechanically working the material. Recovery is the process involving the rearrangement of dislocations into lower energy arrays, without recrystallization [Ref. 14:pp. 363-366]. This results in a boundary misorientation of less than 1 degree, whereas when recrystallization occurs, the misorientation typically exceeds 10 degrees [Ref. 15:p. 192]. Recovery is usually followed by recrystallization and

can be either continuous or discontinuous. Continuous recrystallization forms high angle grain boundaries by subgrain boundary migration and coalescence [Ref. 16], whereas discontinuous recrystallization is a process involving nucleation and growth of new, strain-free grains. The discontinuous recrystallization is relatively rapid [Ref. 16:p. 75], but when suppressed, the misorientation increase of adjacent subgrains via continuous recrystallization results in a finer grain size and has been observed by Nes [Ref. 17:p. 2055], Ahlborn et al. [Ref. 18:p. 944] and Watts et al. [Refs. 19:p. 196; 20:p. 205] in other aluminum alloys exhibiting superplasticity.

Prior to exhibiting superplastic response most of the technologically important alloys require some sort of processing. The three significant variables affecting the superplastic response of this alloy during thermomechanical processing (TMP) have been identified as final true strain, the reduction in thickness during each warm rolling pass, and the length of reheating time between each warm rolling pass [Refs. 21-28]. The observations previously made led to the development of a plan to investigate the effects of changing the three variables. Final rolling true strain was either 1.5 or 2.5, the amount of reduction per pass was either 1 mm or 2.5 mm, and the length of the reheating time between passes was either 4 minutes or 30 minutes. Various combinations of these variable changes yield a number of

comparisons which may potentially isolate the effect of each of the variables.

D. DIFFERENTIAL SCANNING CALORIMETRY

To investigate microstructural evolution of a material the differential scanning calorimeter (DSC) can be used to determine changes that occur. Figure 2.1 schematically shows how the DSC operates. Both the sample of interest and the reference sample are heated or cooled at programmed rates while the differences in power required to maintain the programmed rate are monitored. If the sample of interest requires more power to maintain the programmed heating rate than the reference sample, then the reactions that are occurring in the sample are endothermic; conversely, less power requirement indicates that an exothermic reaction is occurring and releasing energy..

The DSC has been used as an investigative tool that has accurately identified the dissolution, precipitation, and recrystallization [Refs. 29-32] reactions occurring in various alloys. The DSC traces that are produced during a heating (or cooling) run can be used to determine the specific heats or energies of the reactions that are occurring [Ref. 33]. Since the DSC has been used to investigate the differences between alloys [Ref. 34], it should be very informative when specific mechanical processes are compared in the same alloy.

DSC SCHEMATIC

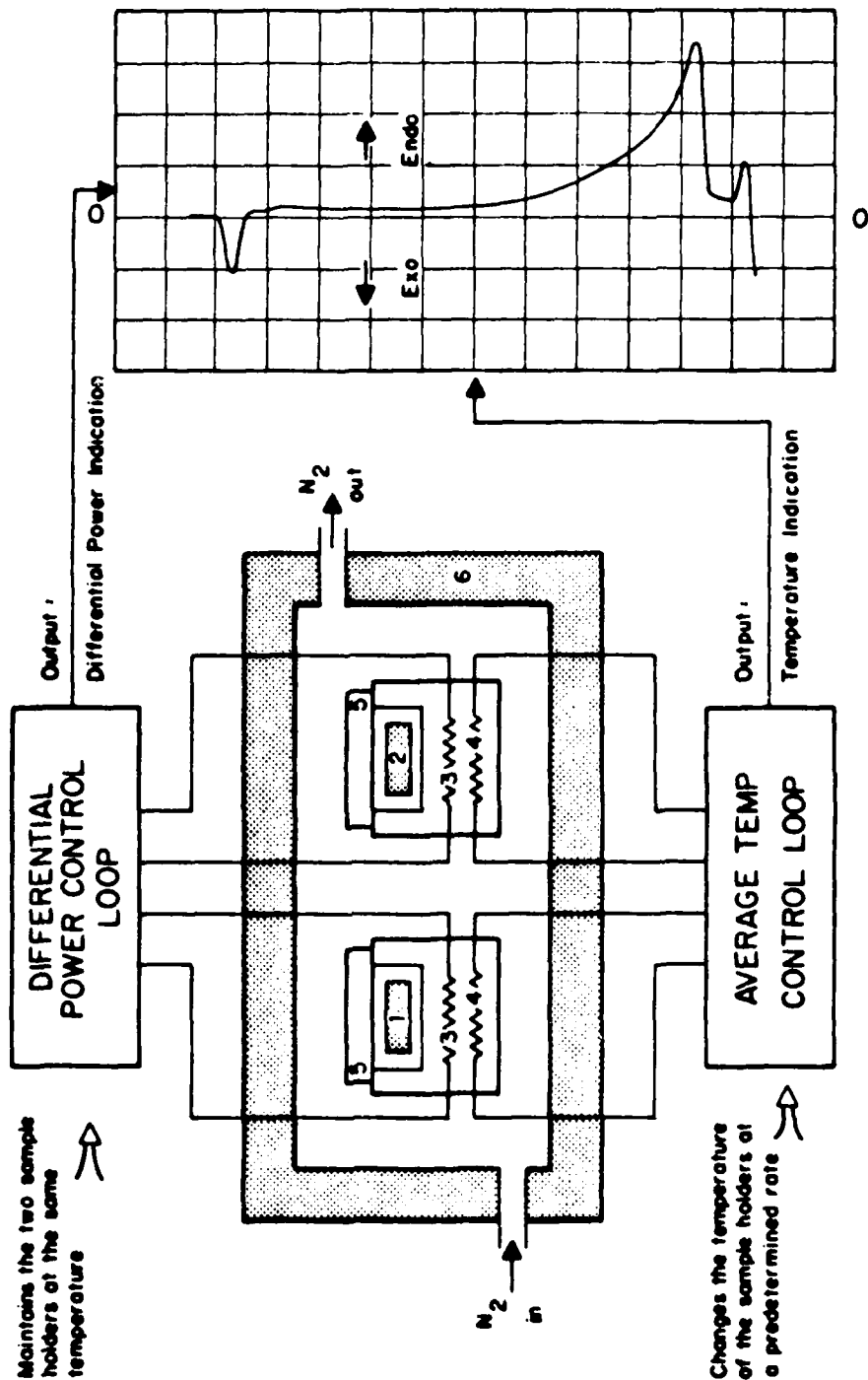


Figure 2.1 Differential Scanning Calorimeter Schematic

E. TRANSMISSION ELECTRON MICROSCOPY

The DSC is capable of identifying microstructural changes that occur, but is not able to distinguish between which type of endothermic or exothermic reaction is occurring. Microscopy has been used in conjunction with the DSC previously [Ref. 35] by using the microscopy to investigate the changes detected by the DSC. The transmission electron microscope (TEM) is able to distinguish between fine microstructural differences and can give an indication of the magnitude of the misorientation between adjacent substructures. This makes the DSC-TEM combination an investigative tool that can yield significant results.

F. SUMMARY

The variety of TMP variable combinations results in a potential experimental matrix that is unmanageable; judicious selection of variables can indicate the effect of each variable. When significant variations in mechanical properties are observed the DSC can detect the nature of the reaction and the temperature at which it occurs. Then, the TEM can be used to accurately identify the microstructural evolution occurring.

III. EXPERIMENTAL PROCEDURE

A. MATERIAL

The nominal composition of the aluminum alloy was reported as Al-10%Mg-0.1%Zr (wt. %). The ALCOA Technical Center, Alcoa Center, Pa, produced the direct-chill cast ingot using 99.99% pure aluminum alloyed with commercially pure magnesium, aluminum-zirconium master alloy, titanium-boron addition to control the as-cast grain size, and, for oxidation control, beryllium as 5% Be aluminum-beryllium master alloy [Ref. 36]. The alloy's chemical composition is shown in Table I.

TABLE I

ALLOY COMPOSITION (WEIGHT PERCENT)

Serial No.	Si	Fe	Mg	Zr	Ti	Be	Al
S572826	0.02	0.02	9.89	0.09	0.01	0.0003	Balance

B. THERMOMECHANICAL PROCESSING

The as-cast ingot was sectioned into billets with a cross section of 31.8 mm (1.25 in.) square and a length of 95.3 mm (3.75 in.). Each billet was then solution treated and upset forged at 440°C which follows the procedure developed by Johnson [Ref. 37], modified by Becker [Ref. 38], and refined, concurrently with Wise [Ref. 28]. This

hot working resulted in a reduction of about 70%, or a true strain of about 1.3.

After upset forging the material was processed differently by warm-rolling and changing the three processing variables as illustrated in Table II. The potential number of different variable combinations was initially reduced to 5, concurrently with Wise [Ref. 28], and then increased to the 6 different processes shown in Table II. The additional process used allowed for an increase in the ability to isolate the effects of each variable. The various processes, TMP1 through TMP6, tabulated in Table II, provide a wide range of comparisons.

TABLE II
THERMOMECHANICAL PROCESSING SCHEDULE

TMP	FINAL ROLLING STRAIN	REDUCTION PER PASS (MM)	REHEATING TIME PER PASS (MIN)	% ELONGATION
1	2.5	1	30	480
2	2.5	2.5	4	260
3	2.5	1	4	470
4	1.5	1	4	168
5	1.5	2.5	4	250
6	2.5	2.5	30	525

C. SAMPLE PREPARATION

Elevated temperature tension test specimens were fabricated as described by Alcamo [Ref. 22]. The samples for use in the DSC were prepared of a size that could also be used in the TEM. Thin disc-shaped specimens were prepared by wafering the as-rolled material, parallel to the long transverse direction, to a thickness of about 0.40 mm; and then further reduction, by a fine grit silicon carbide paper, was accomplished to a thickness of about 0.15 mm. Then, discs of a diameter of 3.0 mm were produced by using a through-type punch.

This size sample was adequate for use in the DSC, weighing about 5 mg. After the information was obtained from the DSC these samples were prepared for investigation in the TEM. Foils for the TEM were prepared by a twin-jet polishing in a Struers Tenupol 2 Electro-Thinning unit. A setting of 15 vdc was used, and a solution of 25% HNO₃ in methanol cooled to -20°C was the electrolyte.

D. MEASUREMENTS AND DATA REDUCTION

1. Tensile Testing

Elevated temperature testing was conducted following the procedures outlined by Becker [Ref. 38] and Hartman [Ref. 24], with minor modification. An Instron Model TT-D with a Marshall Model 2232 three-zone furnace, for temperature control, was used to conduct the testing. The crosshead speeds used in this research ranged from 0.05

mm/min (0.002 in/min) to 127 mm/min (5.0 in/min), which correspond to strain rates ranging from 6.67×10^{-5} 1/sec to 1.67×10^{-1} 1/sec.

Elongation was determined by measuring the marked gage section before and after testing. Percent elongation was determined by measuring the difference between these gage marks and dividing by the initial length. The Instron strip chart measured applied load (lbs.) vs. chart displacement. From the strip chart raw data points of load and chart displacement were taken using the "floating of slope" and computer program (see Appendix A) developed by Grider [Ref. 25]. Data for the peak elongation attained in the tension testing of each TMP are included in Table II.

2. Calorimetry

The calorimetric measurements were taken with a Perkin-Elmer DSC-2C Differential Scanning Calorimeter with a Perkin-Elmer Scanning AutoZero accessory attached. These results were recorded with a two-pen Perkin-Elmer Model 56 strip-chart recorder. The samples of interest were placed in an aluminum pan with an aluminum cover. Since the prepared samples were small enough [Ref. 33], the reference material was simply an aluminum pan and cover, the same one being used for all DSC runs made. The sample and reference holders were kept in a dynamic atmosphere of dry nitrogen flowing at 20 ml/min. The temperature range investigated

was 323K-723K (50°C-450°C) at a programmed rate of 40K/min for both heating and cooling.

Three runs were made for each sample. The DSC trace from the third run was assumed to represent the response of the solution treated condition in which no further microstructural changes would be expected for the heating (and cooling) rates employed. The data for the endothermic and exothermic reactions were obtained by taking the difference between the third trace and the trace of the first run. This is a slight modification to the two-run approach developed by Andrews [Ref. 27]. This change was made to ensure that the data collected reflected the reactions that did occur during the heating cycle. These data were then reduced to heat capacity vs. temperature data as prescribed by the manufacturer [Ref. 33].

E. MICROSCOPY

After the samples had experienced the heating cycles of interest they were prepared for examination in the transmission electron microscope, as described in Section C of this chapter. A JEOL JEM-100CX II transmission electron microscope was used to examine the microstructure and produce the micrographs presented in this work. The accelerating voltage used throughout this work was 120 kV.

IV. RESULTS AND DISCUSSION

This chapter will report the results obtained in this research on the effect of the three thermomechanical processing variables on superplasticity. Three distinct areas of results are: first, mechanical properties observed in tensile testing; second, differential scanning calorimeter (DSC) measurements of the energies involved in various reactions that occur in the samples when they are heated to elevated temperatures; and, third, transmission electron microscopy (TEM), to characterize the microstructural evolution that occurs in heating to elevated temperatures.

A. MECHANICAL PROPERTIES

Mechanical testing at elevated temperatures was conducted to investigate the deformation characteristics of processes TMP1 through TMP6. As previously described in Chapter III, tension testing was conducted at 300°C while varying nominal strain rates from 6.67×10^{-5} 1/Sec to 1.67×10^{-1} 1/Sec. The stress vs. strain results of the tension tests are presented graphically in Figure 4.1 for TMP2 and the stress vs. strain plots for the other processes are included in Appendix B. The data for the true stress observed at 0.1 plastic strain and the percent elongation as a function of strain rate will be presented throughout this chapter. The

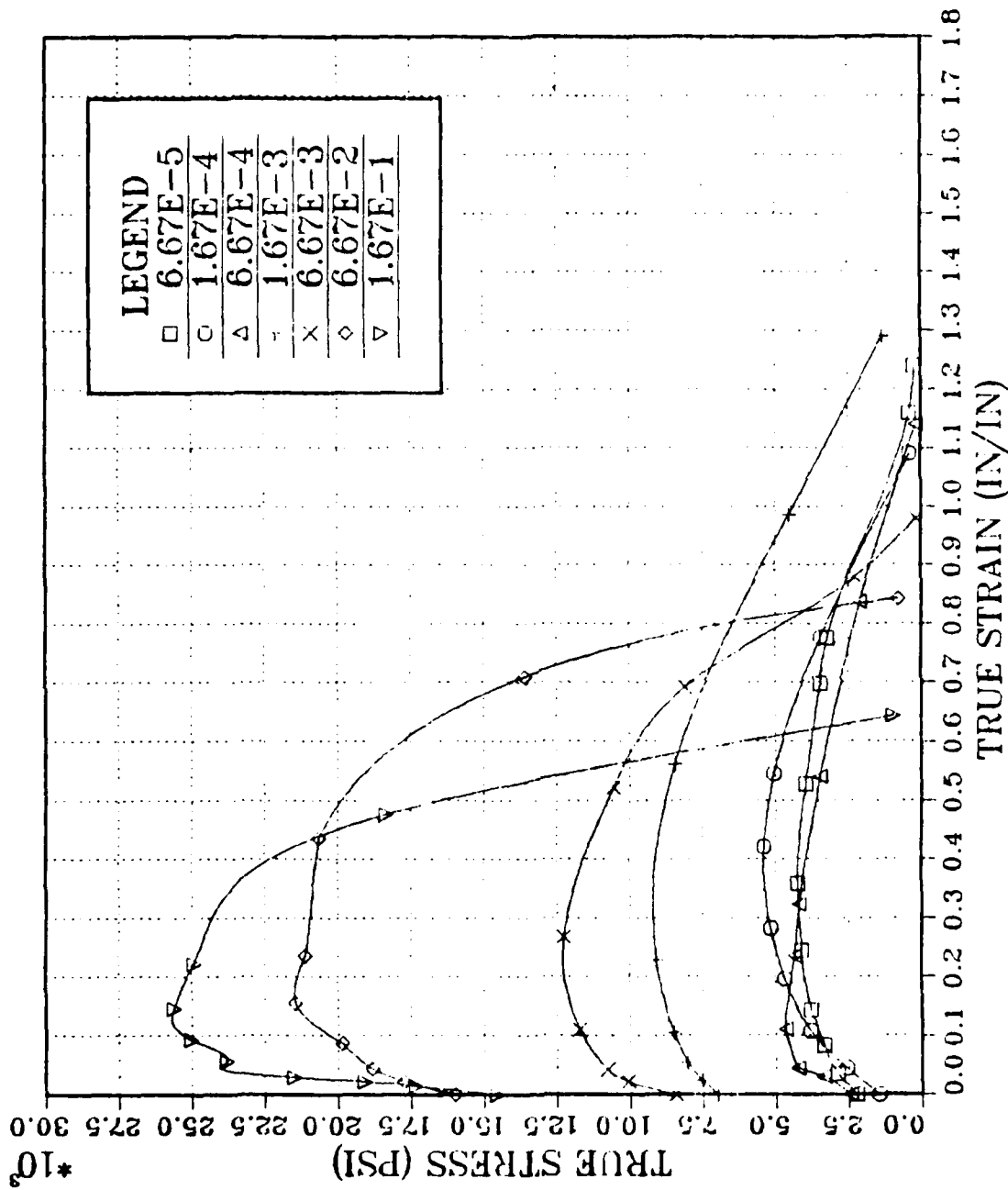


Figure 4.1 True Stress vs. True Strain Plot for Tensile Testing Conducted at 300°C for an Al-10Mg-0.1Zr Alloy. The Specimen was Heat Treated and Upset Forged as Described in This Work and Warm Rolled Using Schedule TWP2 Described in Table II

three processing variables investigated were total rolling strain, reheating time between each pass during rolling, and the reduction per pass.

1. Effect of Total Rolling Strain (1.5 vs. 2.5)

The two different nominal strains investigated were 1.5 and 2.5. As indicated in Table II, TMP4 and 5 represent warm rolling to a final true strain of 1.5, while TMP1, 2, 3, and 6 represent warm rolling to a final true strain of 2.5. From Table II it is seen that the effect of final true strain may be observed by comparing TMP3 and TMP4 for 1 mm reduction per pass, and by comparing TMP2 and TMP5 for 2.5 mm reduction per pass.

In Figure 4.2a the effect of increasing total rolling strain from 1.5 to 2.5 seems to produce only a slight increase in ductility. Figure 4.2b supports the observed differences in ductility with the large, 2.5 mm per pass reduction, as it shows TMP2 to be weaker than TMP5 as well as more ductile. The second comparison of increasing total true strain (TMP3 versus TMP4) shows an effect that is much more pronounced with the smaller, 1 mm reduction per pass. Figure 4.3a shows that increasing the final true strain results in a significant increase in ductility for the range of strain rates from 6.0×10^{-4} to 3.0×10^{-2} 1/Sec. Figure 4.3b shows a similar strength as when TMP2 and TMP5 were compared.

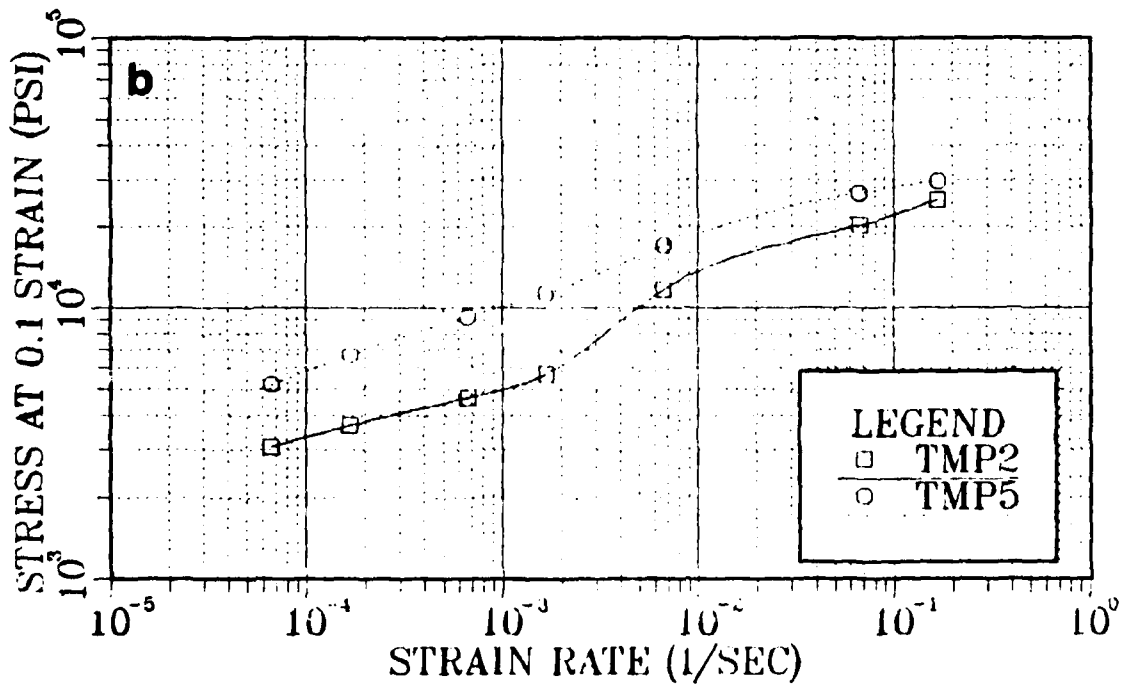
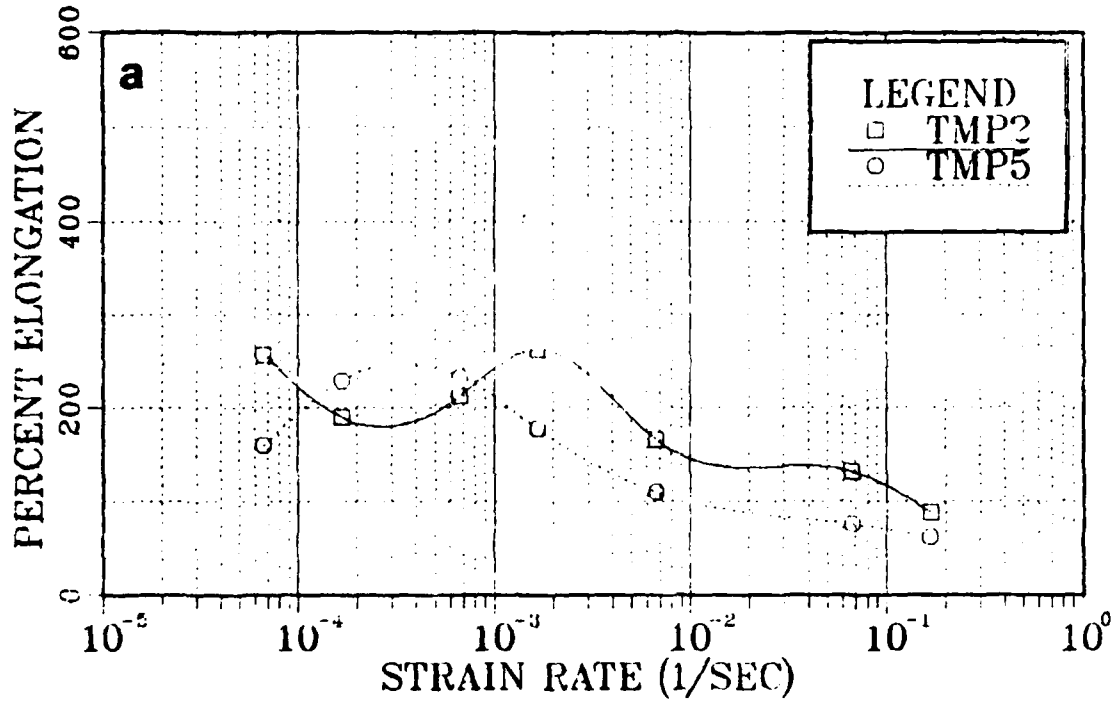


Figure 4.2 Graph of (a) Percent Elongation vs. Log Strain Rate and (b) Log True Stress vs. Log Strain Rate for TMP2 and TMP5

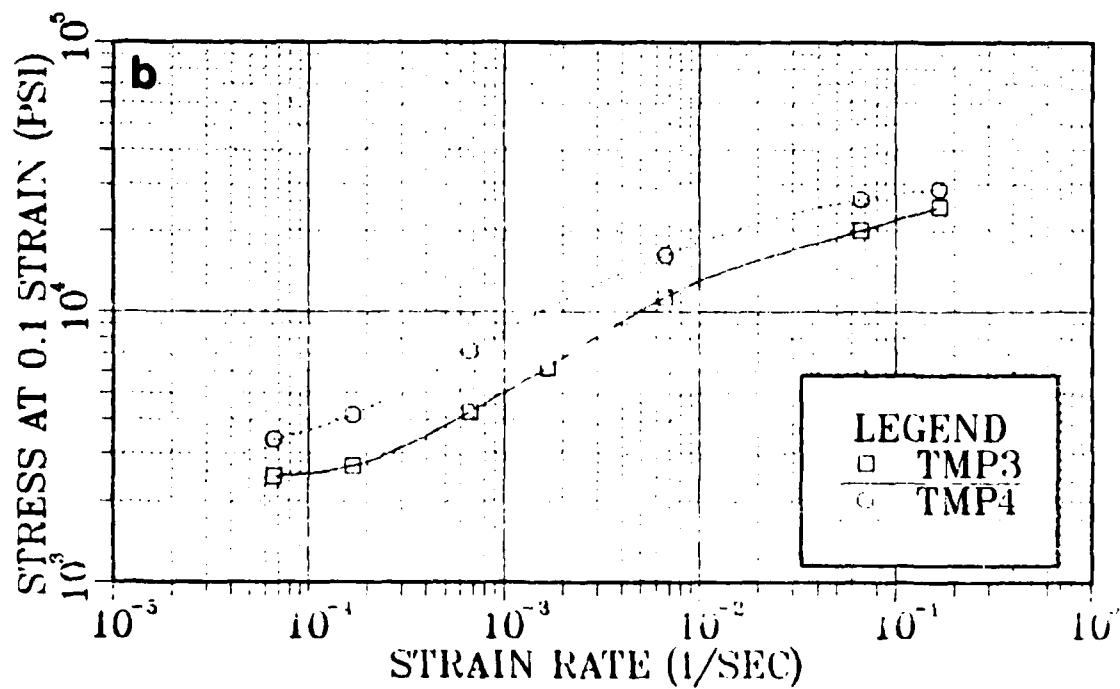
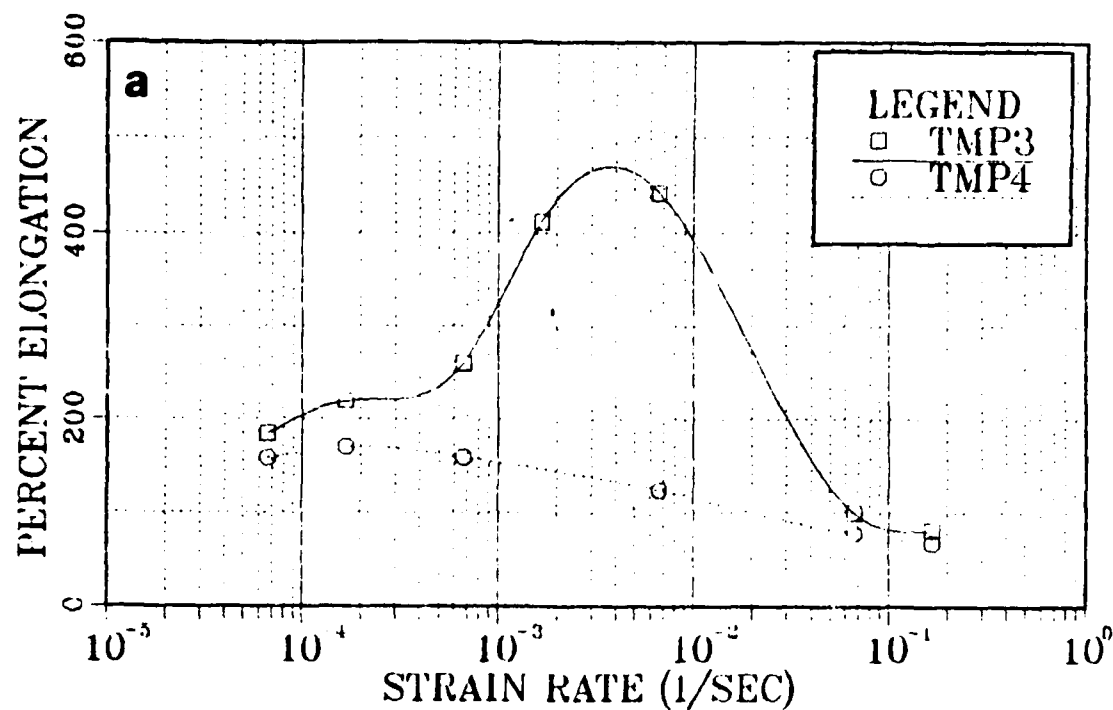


Figure 4.3 Graph of (a) Percent Elongation vs. Log Strain Rate and (b) Log True Stress vs. Log Strain Rate for TMP3 and TMP4

From these comparisons the actual effect of final true strain cannot be accurately isolated. In each case the increase in final true strain showed both an increase in ductility and a decrease in strength. However, the magnitude of the ductility enhancement of the smaller reduction scheme (TMP3 and TMP4) is much greater than for the large reduction process (TMP2 and TMP5). The primary difference between these comparisons is that TMP3 and TMP4 have experienced more time at the warm rolling temperature than TMP2 and TMP5. Consequently, the next variable that will be investigated is the reheating time between each warm rolling pass.

2. Effect of Reheating Time Between Passes (4 vs. 30 Min)

Two values of reheating times between warm rolling passes were investigated: 4 minutes and 30 minutes. Comparison of Figures 4.4 and 4.5 reveals that the increase in reheating time between passes resulted in significant changes in ductility and strength.

In the 1 mm per pass processes (Figure 4.4) the increased reheating time between the passes caused the peak ductility to increase very slightly (from 470% to 480%). With increased reheating time, however, there is a significant ductility increase seen at lower strain rates and also a much wider range of strain rates over which superplastic behavior was observed. The 2.5 mm per pass processes (Figure 4.5) similarly showed a wide strain rate range over

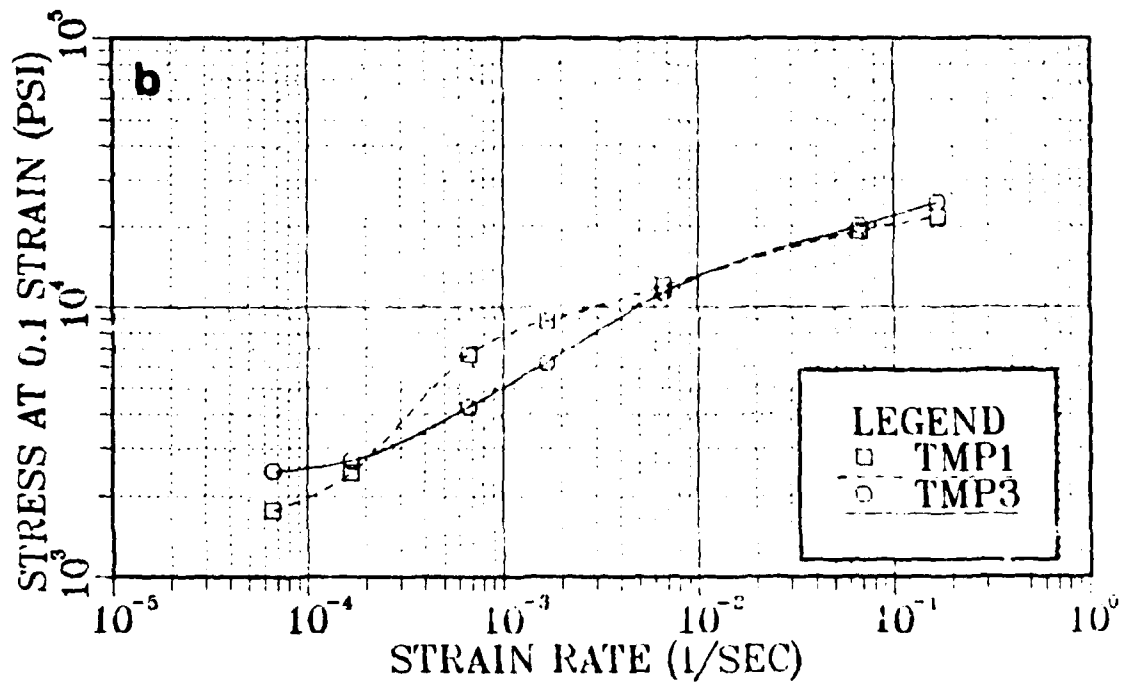
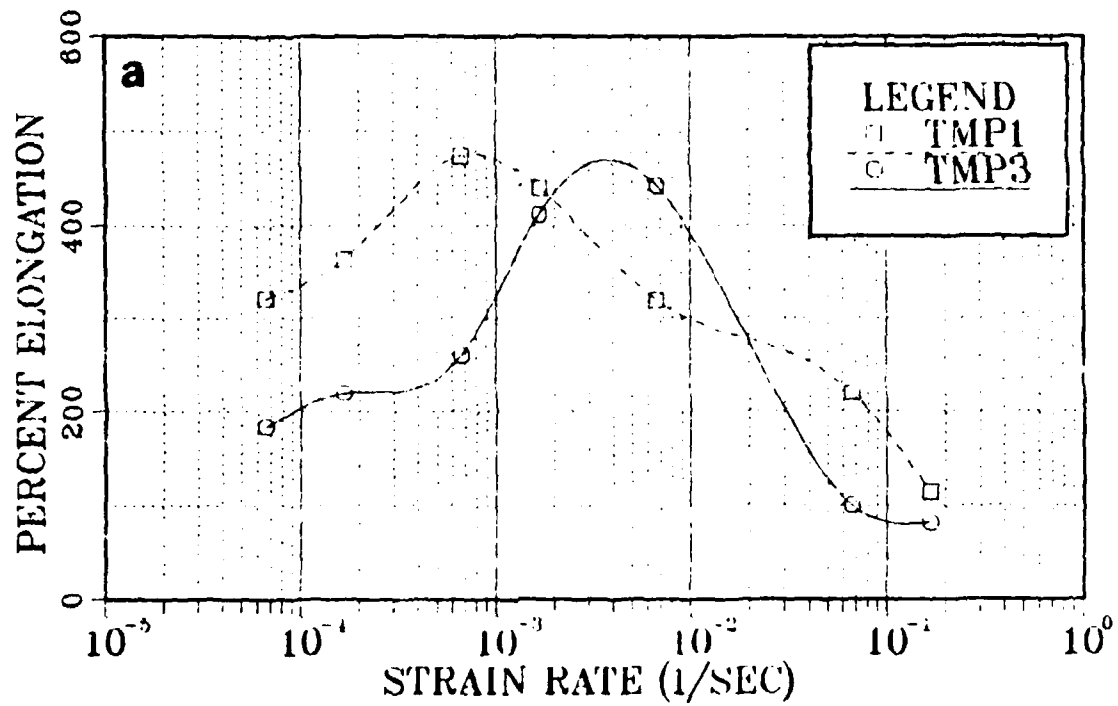


Figure 4.4 Graph of (a) Percent Elongation vs. Log Strain Rate and (b) Log True Stress vs. Log Strain Rate for TMP1 and TMP3

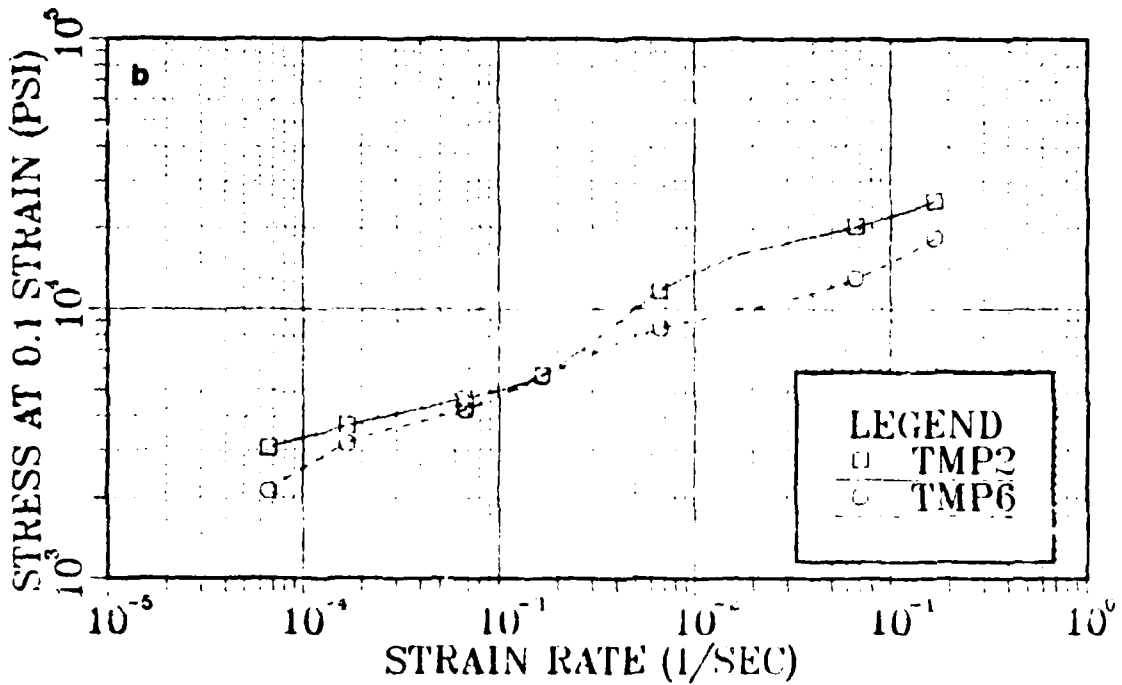
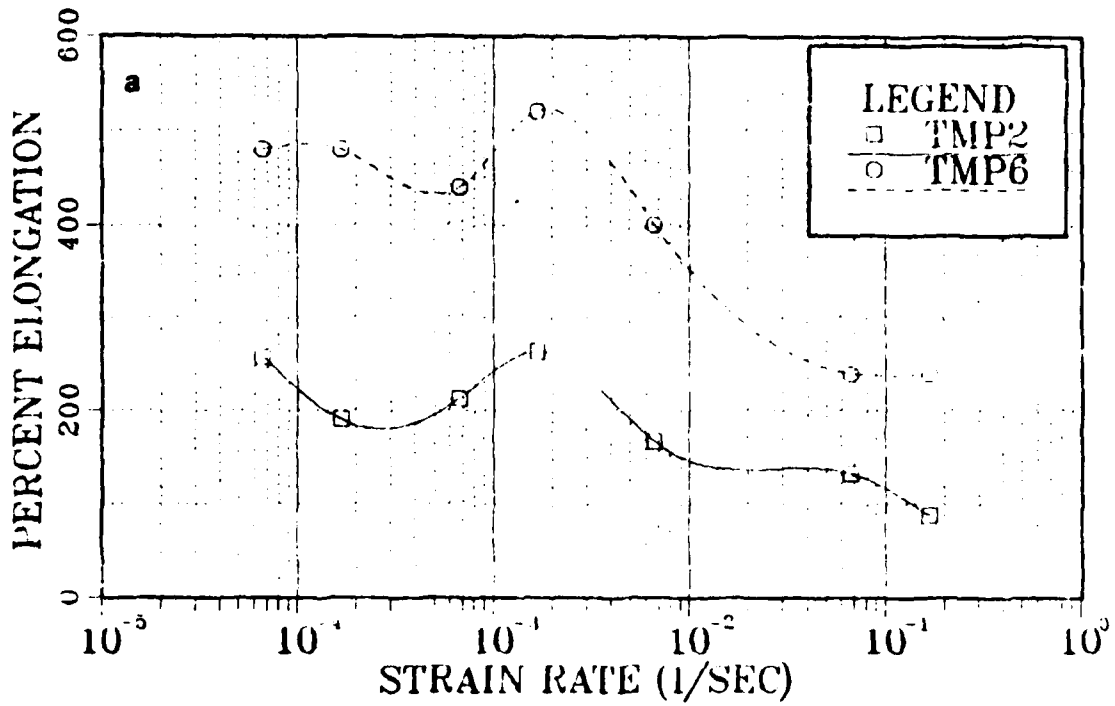


Figure 4.5 Graph of (a) Percent Elongation vs. Log Strain Rate and (b) Log True Stress vs. Log Strain Rate for TMP2 and TMP6

which superplastic behavior was observed when reheating time was increased. However, the most significant shift due to the increased reheating time was a dramatic increase in ductility over the entire range of strain rates investigated. The magnitude of the increase in ductility when TMP2 and TMP6 are compared suggests that the reheating time between each warm rolling pass is the most significant variable. Since there is the additional variable of the total time which the sample has experienced the rolling temperature, seen when Figures 4.4 and 4.5 are compared, it is apparent that when the reduction per pass is increased the length of reheating time between each pass must also be increased to obtain the superplastic behavior desired. Also, the third variable, reduction per pass, needs to be isolated and investigated.

3. Effect of Reduction Per Pass (1 mm vs. 2.5 mm)

The two different reductions per pass investigated were 1 mm and 2.5 mm. When the reduction per pass is increased from 1 mm to 2.5 mm (at 4 minutes reheating time) the ductility is dramatically decreased (Figure 4.6). However, when the reheating time is increased to 30 minutes the greater reduction per pass condition (TMP6) shows a slight increase in ductility (Figure 4.7a) and exhibits lower strength (Figure 4.7b) when compared to the lesser reduction per pass condition (TMP1). This indicates, again, that the most significant variable considered is the

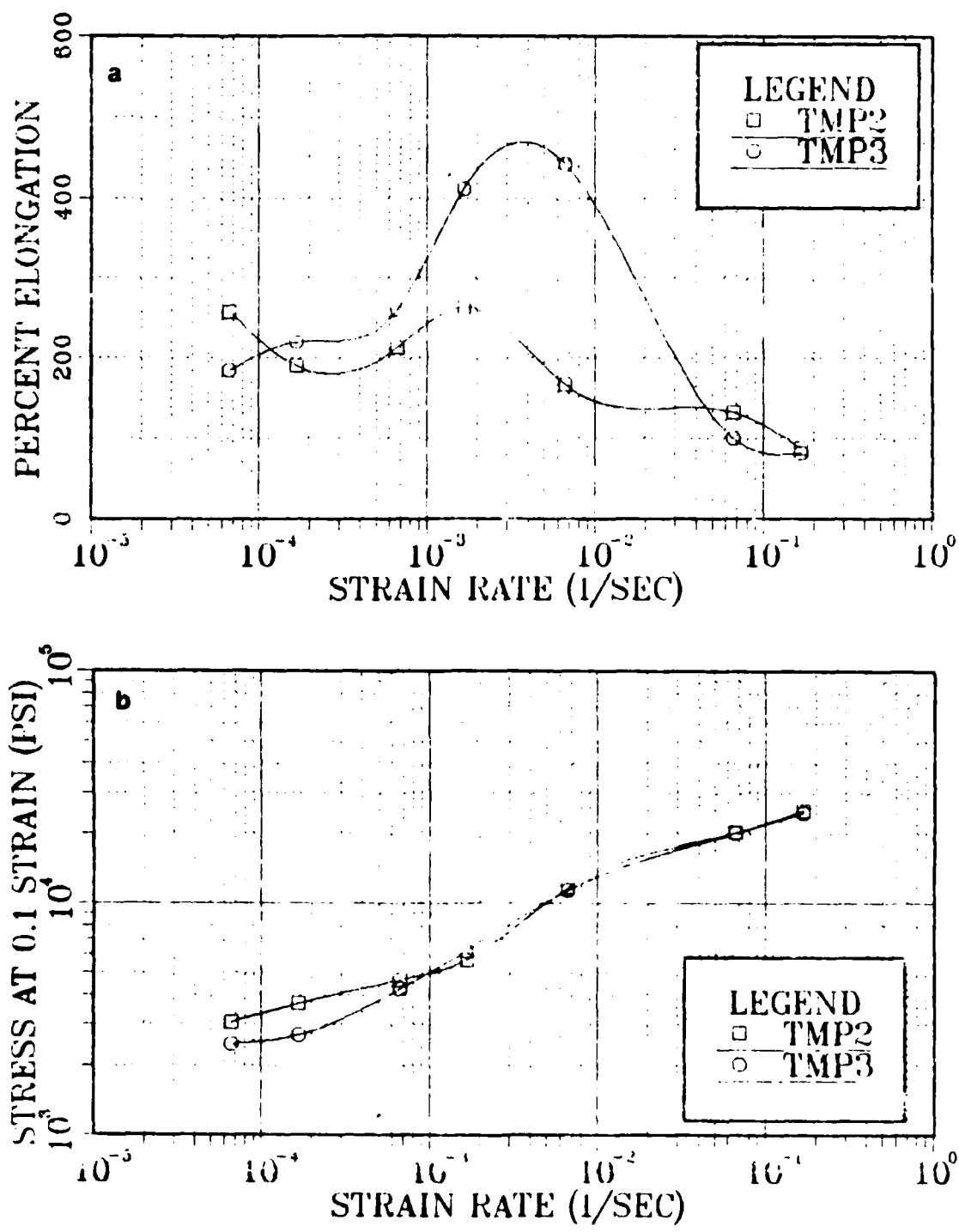


Figure 4.6 Graph of (a) Percent Elongation vs. Log Strain Rate and (b) Log True Stress vs. Log Strain Rate for TMP2 and TMP3

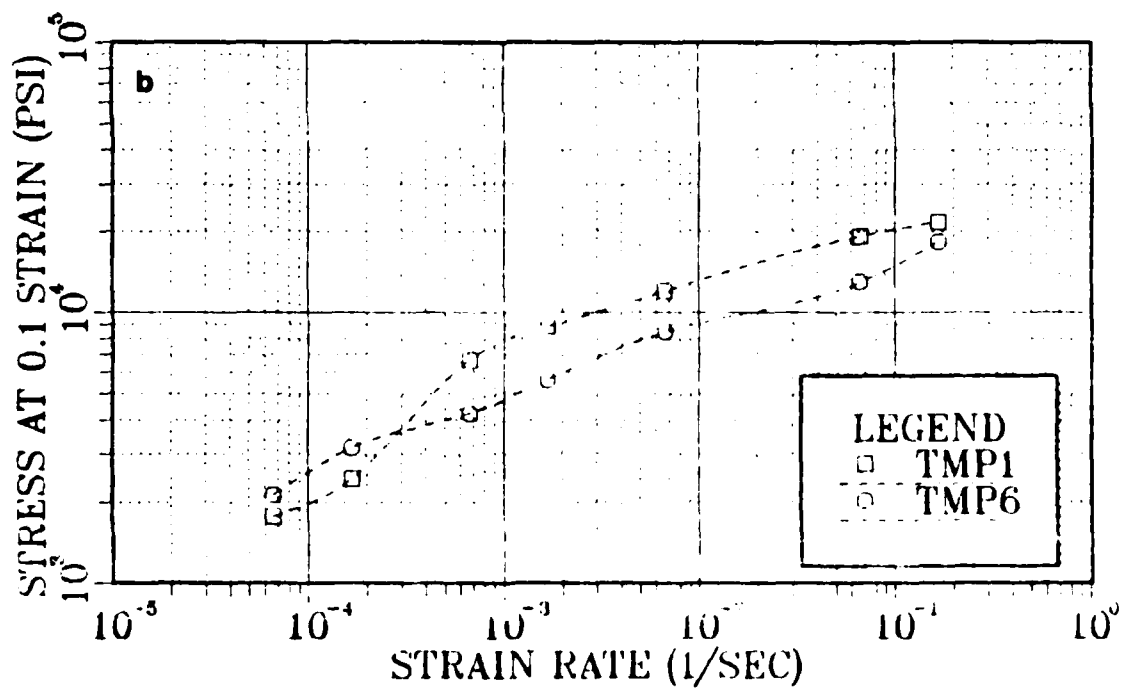
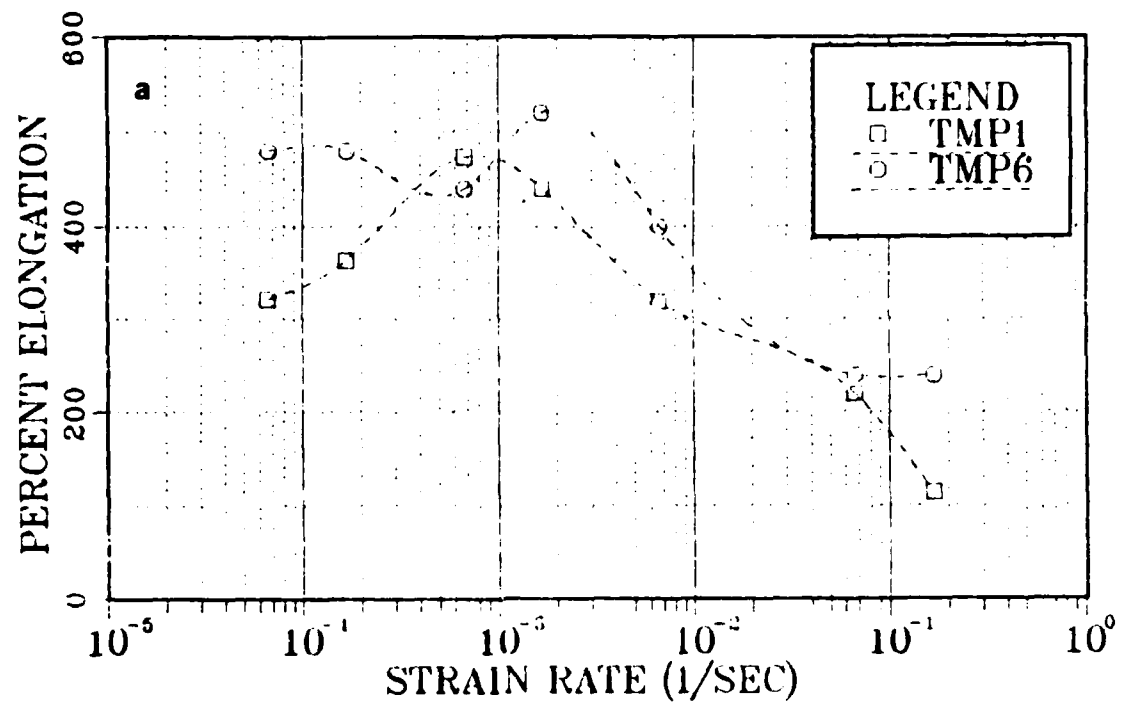


Figure 4.7 Graph of (a) Percent Elongation vs. Log Strain Rate and (b) Log True Stress vs. Log Strain Rate for TMP1 and TMP6

reheating time between warm rolling passes. When Figure 4.6a is compared to Figure 4.7a it is obvious that to obtain superplastic behavior with large reductions per pass, the reheating time between passes must also be increased.

4. Summary

Each of the three variables investigated cause discernible shifts in ductility. Increasing the total true strain from 1.5 to 2.5 caused an increase in the ductility. This increase was much more pronounced in the material that was reduced by 1 mm per pass than in the samples reduced by 2.5 mm per pass. Increasing the reheating time from 4 to 30 minutes caused a significant increase in ductility over a wide range of strain rates. These increases were much more significant in the material that was reduced by 2.5 mm per pass than the samples reduced by 1 mm per pass. Increasing the reduction per pass from 1 mm to 2.5 mm caused a decrease in ductility in the material that was allowed 4 minutes reheating time between passes, but caused an increase in ductility in the samples that were reheated 30 minutes between passes. All of these observations indicate that superplastic response may be obtained to differing degrees by varying final true strain, reheating time between passes and the amount of reduction per pass.

The specific effect of each variable on superplastic response cannot be isolated and studied independently. However, the single most important variable appears to be

the reheating time between warm rolling passes. In each case when the amount of strain a sample experiences is increased, the superplastic response is enhanced when the amount of reheating time is also increased.

Superplasticity is enhanced by grain refinement. Grain refinement in these Al-Mg alloys has been proposed [Ref. 39] to result from continuous recrystallization of an initially non-recrystallized microstructure. This is essentially a recovery process, i.e., the initially high dislocation density recovers to form subgrain boundaries which coalesce in turn to form higher misorientation boundaries. This process was thought to occur mainly during the heating prior to superplastic testing and in response to the large dislocation densities attained in the penultimate and final passes. Thus, combinations of processing variables which raise the number of dislocations available for continuous recrystallization should result in a refined grain size and enhanced ductility. This is, in fact, observed for total rolling strain; increased strain resulted in increased subsequent superplastic ductility. Also, larger reductions per pass result in enhanced superplastic ductility, especially at the longer reheating times.

A short reheating time should also aid in retaining a high dislocation density to provide for finer recrystallized grains. This was not observed; a longer reheating time generally resulted in higher superplastic ductility or

in broader strain rate ranges for such ductility. This result can only be interpreted in terms of a model including continuous recrystallization during the warm rolling process and requiring time in excess of four minutes between passes for the heavier reduction per pass materials.

A high dislocation density alone, in conjunction even with prolonged annealing after the completion of rolling, is not sufficient; as noted by Grider [Ref. 25], a process including large reduction per pass, large total strain and a short reheating time was only marginally superplastic and annealing for one hour at 300°C resulted in little apparent improvement in ductility. The data of this research show clearly that similar total time at temperature with the more lengthy reheating time between warm rolling pass will result in a much improved superplastic ductility. The subsequent analyses by DSC (Differential Scanning Calorimetry) and TEM (Transmission Electron Microscopy) are intended to assess further this conclusion.

B. DIFFERENTIAL SCANNING CALORIMETRY

Due to the number of variables investigated, several comparisons of results were developed. The significant effects of each processing variable identified in the mechanical testing stage of this research were discernible, but not quantifiable. The Differential Scanning Calorimeter (DSC) was chosen as a second investigative tool to be used to further understand the effects of the processing

variables. In the DSC the microstructural events that occur during heating can be identified as either endothermic or exothermic reactions. Consequently, when a reaction occurs within the microstructure of the material (like recovery, recrystallization or second phase dissolution) the DSC will be able to detect these changes and produce results that indicate how the magnitude of each effect varies between the differently processed materials. The plots of the data obtained from the processes investigated by the DSC are included in Appendix C.

The first point noted was that there was an endothermic peak observed in all of the five differently processed materials investigated. Process TMP5 was not included in the DSC investigation because the low final true strain samples were only marginally superplastic. Each of the peaks occur within a relatively narrow temperature range (355°C to 390°C) which indicates that a significant portion of the energy absorbed by the sample is used for the dissolution of the β phase. This observation is supported by the fact that the reported solvus temperature for the β phase is about 360°C in a 10 pct Mg Al-Mg alloy [Ref. 7]. The positions of the endothermic peaks are indicative of the approximate temperature at which a transition occurs [Ref. 33], the observed peaks indicate that a transition occurs at about 360°C. Additionally, similar endothermic peaks have been reported [Refs. 31,32,34,39] within this temperature

range for a variety of aluminum alloys. Each of these authors report the reason for the endothermic peaks to be the dissolution of precipitates. Comparing these results with Figure 4.8 indicates that a β phase solvus temperature of 360°C is reasonable since this is near the solvus temperature of a binary Al-10 Mg alloy, about 360°C.

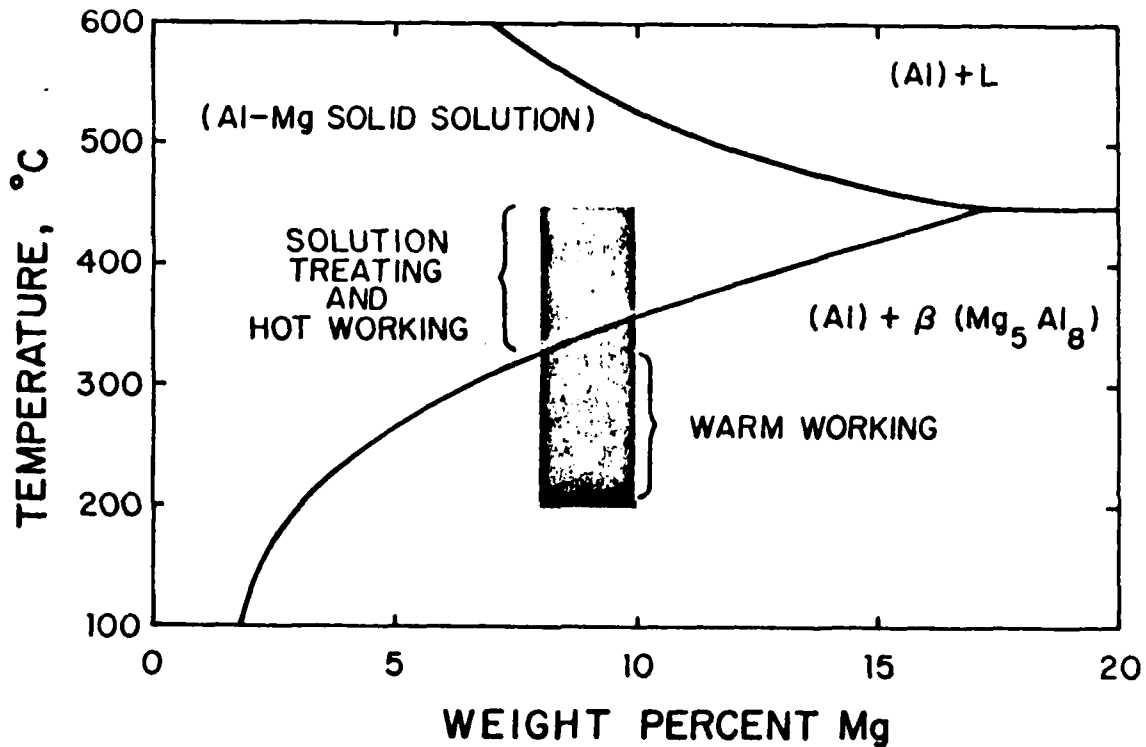


Figure 4.8 Partial Aluminum-Magnesium Phase Diagram with TMP Region Indicated

1. Effect of Total Rolling Strain (1.5 vs. 2.5)

The first comparison considered, as in the previous section, is the effect of total true strain the material has experienced during the warm rolling. Increasing the total strain increases the dislocation density so that when the

elevated temperature testing is performed the recovery and the continuous recrystallization that occurs at the test temperature should cause the production of a fine microstructure. Since recovery and recrystallization are energy-releasing reactions, the DSC will indicate that an exothermic reaction is taking place. A fine microstructure results in a large number of grains and since superplasticity is exhibited via grain boundary sliding, the microstructure should be able to support superplastic ductilities if the microstructure is also stable. This microstructural stability can be seen, in a relative sense, when the magnitudes of the areas under the exothermic peaks are compared.

The increased total strain may be so severe that significant microstructural damage may be introduced by the cracking of the hard Al_3Zr precipitates, as proposed by Wise [Ref. 28], which then provide sites for cavitation and subsequent early failure during the tension test. This type of microstructural damage is not representable as an endothermic or exothermic reaction and cannot be detected by using the DSC. Consequently, this investigation is limited to the actual, observable changes in energy required by or provided by the microstructural evolution upon heating. In Figure 4.9 a comparison of the effect of increasing the final true strain from 1.5 (TMP4) to 2.5 (TMP3) shows that this increased strain increases somewhat the amount of

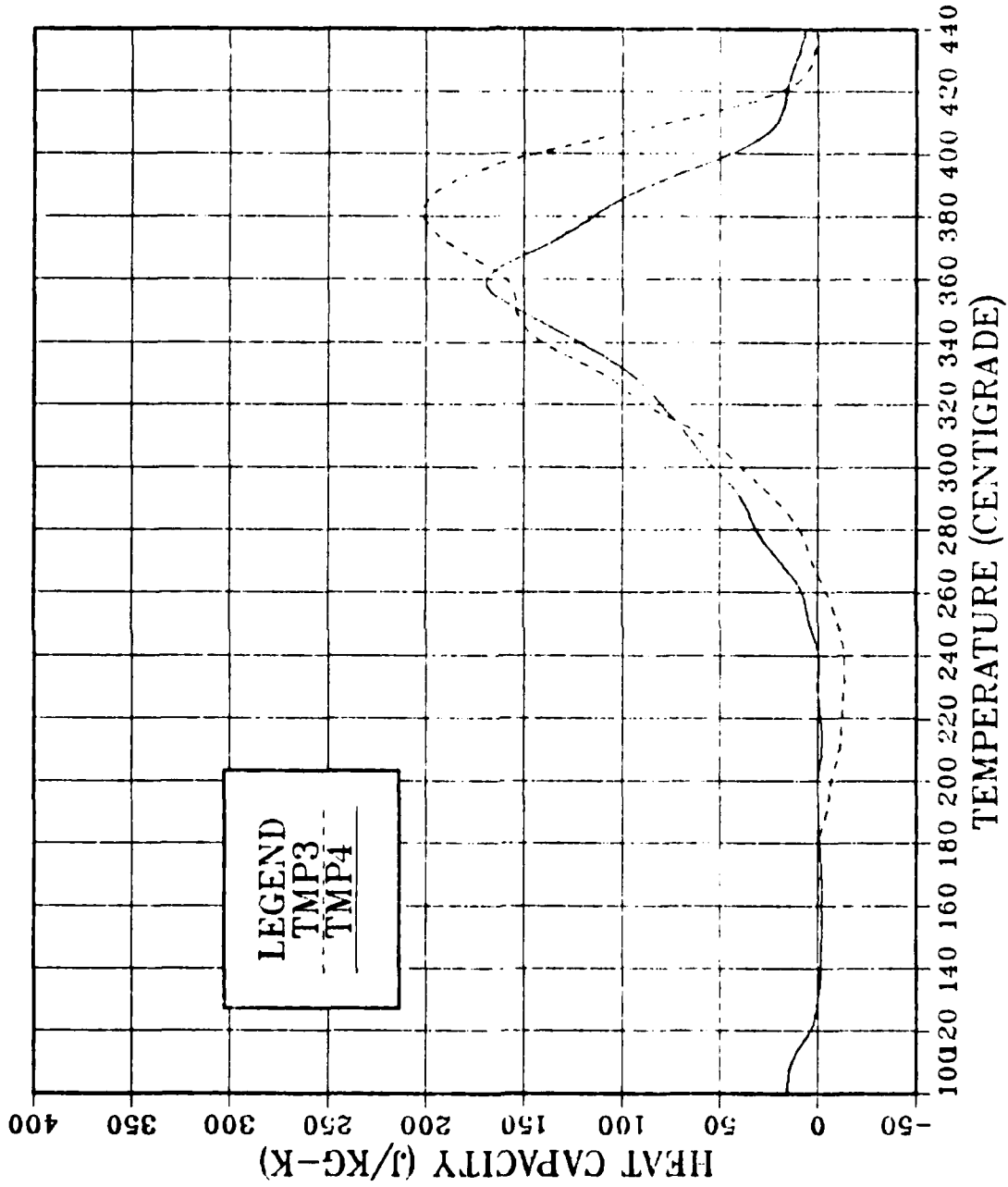


Figure 4.9 Graph of Heat Capacity vs. Temperature for Processes TMP3 and TMP4

endothermic energy required to drive the reactions that occur in the sample during heating. The magnitude of this increase possibly could be related to increased stability or to differing amounts of intermetallic β (Al_8Mg_5) precipitated. Also, TMP3 exhibits a slight exothermic reaction which may indicate recovery during heating at temperatures up to the rolling temperature. Further investigations are limited primarily to the effects of other variables on the samples that have experienced a final, nominal, true strain of 2.5.

2. Effect of Reduction Per Pass (1 mm vs. 2.5 mm)

The effect of increasing the reduction per pass was beneficial for the shorter reheating time, according to the ductility data presented previously. If these differences are caused by an evolution of the microstructure during heating to the tensile test temperature, then the DSC should be able to identify at what temperature the changes occur. Differences are observed when TMP2 and TMP3 are compared, as shown in Figure 4.10. TMP2 exhibits an endothermic peak at about 355°C followed by a smaller peak at about 385°C. A different situation is observed in TMP3, which exhibits a plateau at 355°C and a significant endothermic peak at about 385°C. Andrews [Ref. 27] reported the same results when a similar comparison was made between large reduction material and a lightly reduced material. These results are consistent since the only difference between TMP2 and TMP3

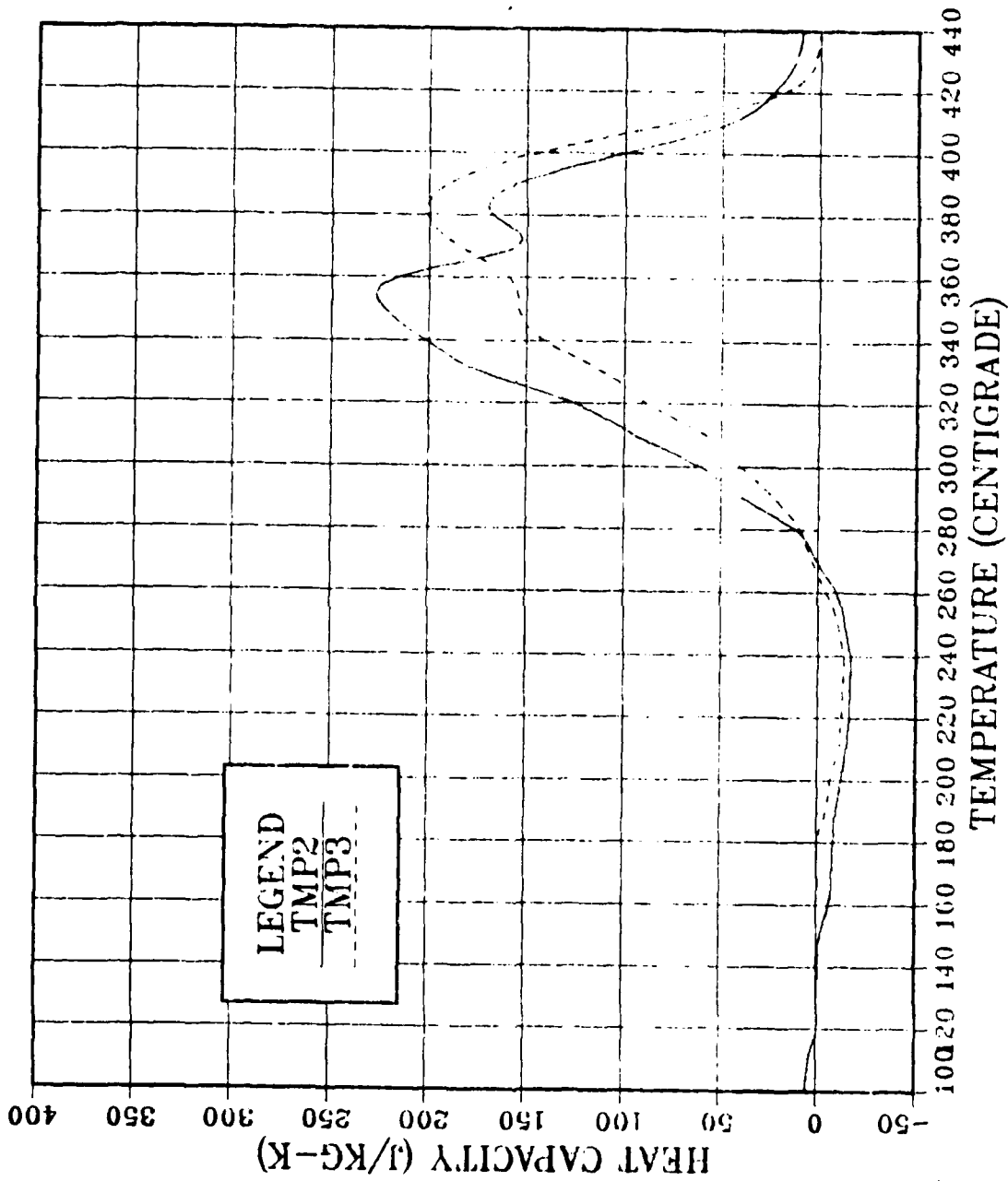


Figure 4.10 Graph of Heat Capacity vs. Temperature for Processes TMP2 and TMP3

is that TMP2 was reduced 2.5 mm on each warm rolling pass (more heavily reduced) whereas TMP3 was reduced only 1 mm per pass (light reduction).

Since the areas under both curves are similar, one would expect the microstructures to be comparable and resultant superplastic responses the same. However, TMP2 had a peak ductility of 260% and TMP3 had a peak ductility of 470%, indicating that the area under the DSC curves are not conclusive as a tool in predicating the potential for superplastic ductilities.

The suggestion by Andrews [Ref. 27] to account for the variations in the endothermic peaks was that there may be a morphological difference in the phase produced by the different processes. Although the establishment of the composition or morphology of the phase is beyond the scope of this work, the additional experimental work with TMP2 and TMP3, shown in Table III, consisting of annealing (TMP200 and TMP300) and recrystallization at 440°C followed by aging at 300°C (TMP240 and TMP340), indicate that a difference does exist between the unprocessed material and the material that has experienced a thermomechanical process. Figure 4.11 shows that the rolled and annealed material has endothermic peaks at 370°C (TMP300) and 380°C (TMP200) at about 345-350 J/kg-K, whereas the rolled, recrystallized and aged materials have endothermic peaks at 405-410°C of 320 J/kg-K (TMP340) and 345 J/kg-K (TMP240). The shift of the

TABLE III
HEAT TREATMENT SCHEDULES FOR TMP2 AND TMP3

TMP	PROCESS	TIME AT 440° (HR)	TIME AT 300°C (HRS)
2	200	0	42
2	240	2	40
3	300	0	42
3	340	2	40

peaks in each TMP is about 30°C, which is significant enough to indicate that there is a distinct difference between the rolled and the undeformed materials. This difference is most likely due to differences in the β phase, either in morphology or a metastability of the deformation-induced β when compared to the thermally-induced β .

This apparent difference in the type of β requires further investigation. To try to identify differences in the precipitates the two previously mentioned heat treatments (annealed at 300°C for 42 hours and recrystallized followed by aging at 300°C for 40 hours) were compared (Figures 4.12 and 4.13). These comparisons show that a proposal to deconvolute the doublet endothermic peaks observed in TMP2 and TMP3 into two separate curves is not unreasonable since they appear as though they could result from some combination of the two different types of the β precipitate. The plots of the heat treated materials appear to include a different portion of the curves resulting from

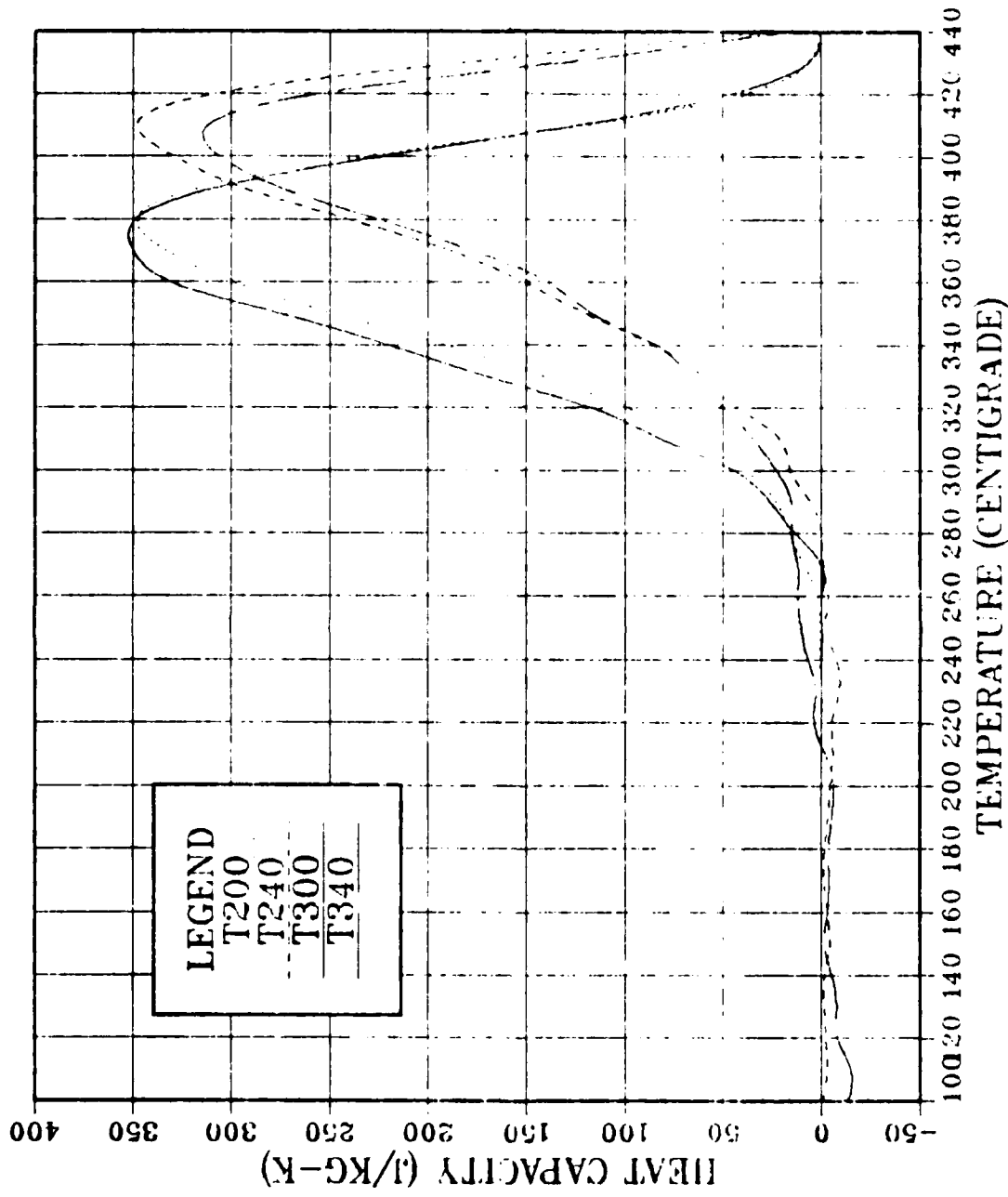


Figure 4.11 Graph of Heat Capacity vs. Temperature for Processes T200, T240, T300 and T340

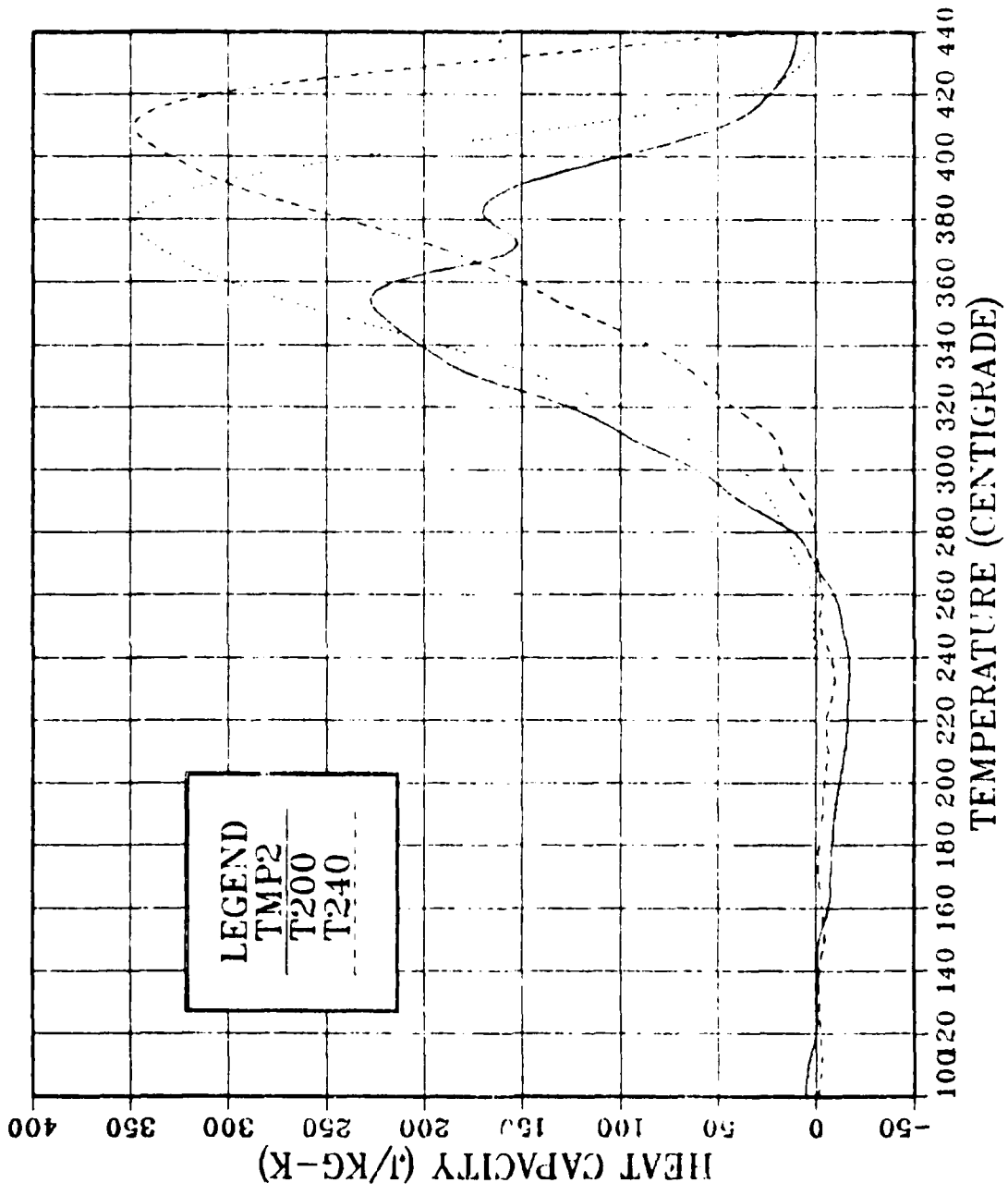


Figure 4.12 Graph of Heat Capacity vs. Temperature for Processes TMP2, T200 and T240

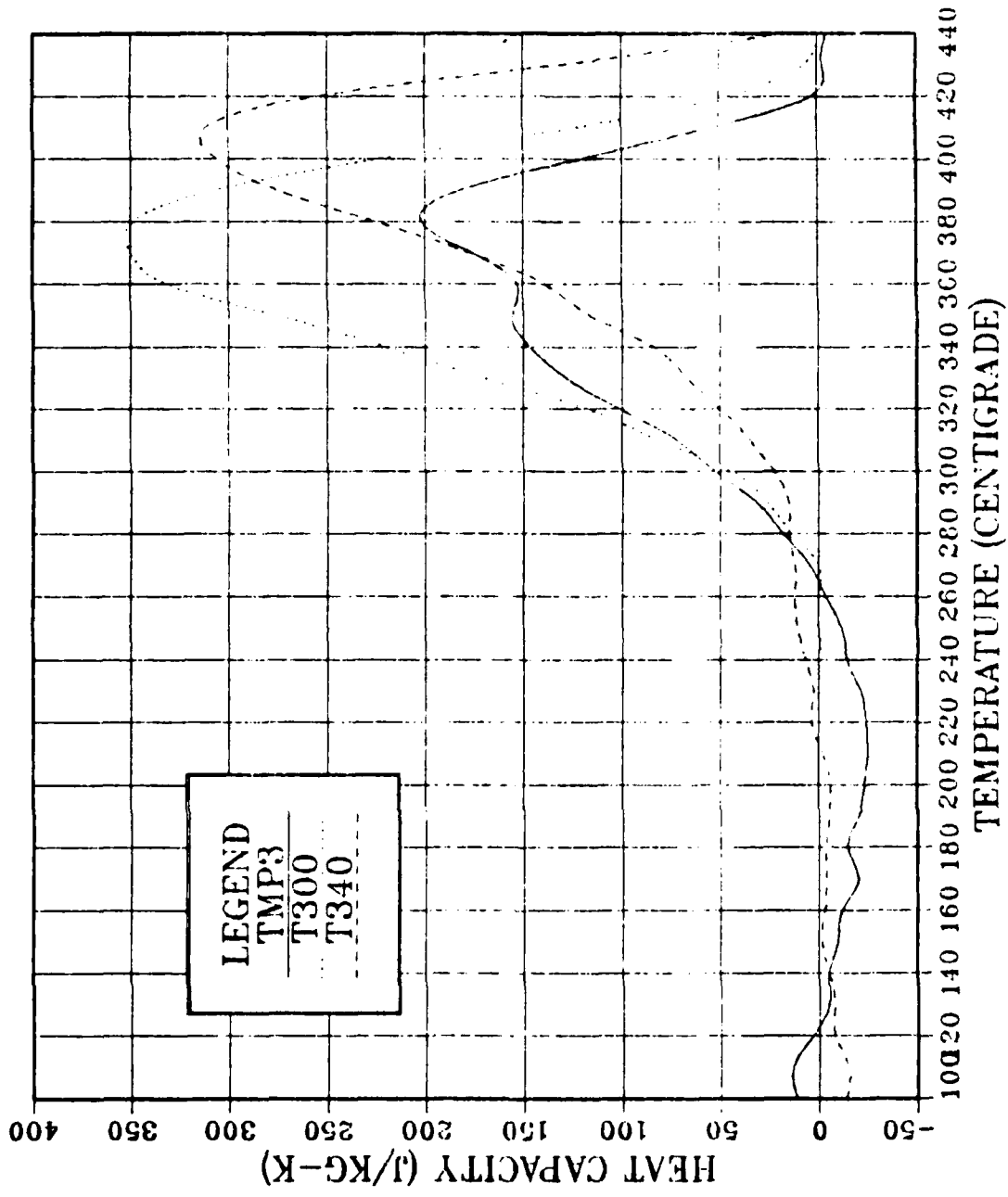


Figure 4.13 Graph of Heat Capacity vs. Temperature for Processes TMP3, T300 and T340

the as-rolled materials. So the possibility exists that the production of either of these as-rolled plots could be accomplished by combining two separate endothermic dissolution reactions, which is possibly attributable to the deformation-induced and the thermally-induced β , and some combination of exothermic reactions (recovery and either continuous or discontinuous recrystallization).

An additional comparison of the effects of reduction per pass is available when a comparison of the DSC plots for TMP6 (large reduction) and TMP1 (small reduction) are made, as shown in Figure 4.14. In both of these cases there are two endothermic peaks, as also observed in TMP2 and TMP3. The major difference seen when TMP6 and TMP1 are compared is that the magnitude of the lower temperature endothermic peaks are significantly less than the peaks observed at the higher temperature. The fact that the two different endothermic peaks exist in each case supports the proposition that superposition of the effects of the differing β phase morphology or its metastability and various exothermic reactions are potentially the cause of the doublet peak curve shape.

The significant and consistent observation noted is that the second endothermic peak of the heavy reduction material occurs at higher temperatures and are of a lesser magnitude in each comparison. This indicates that the most significant contribution of the reduction per pass is that,

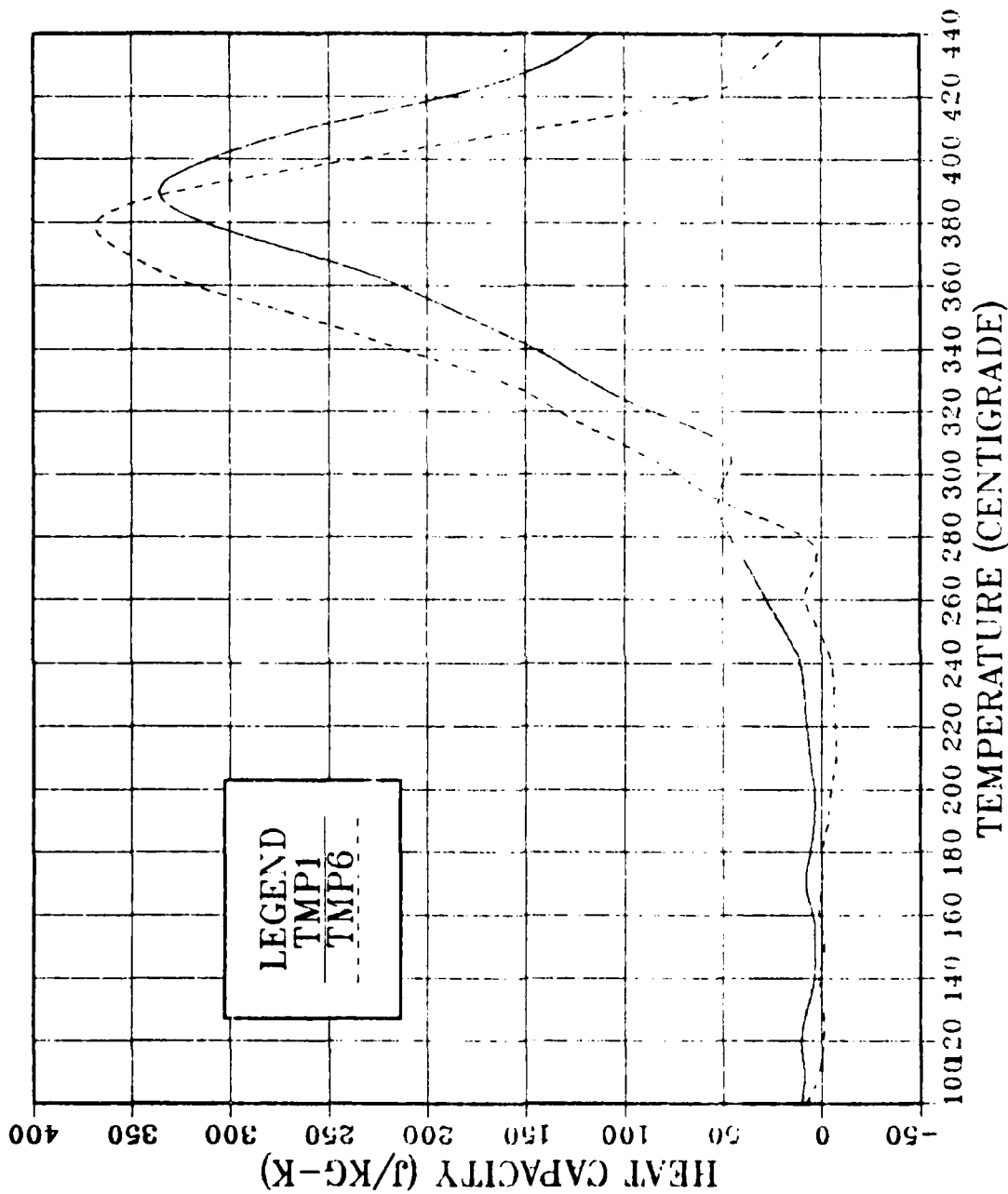


Figure 4.14 Graph of Heat Capacity vs. Temperature for Processes TMP6 and TMP1

as the reduction per pass is increased, the second of the endothermic peaks occurs at a higher temperature and the amount of energy to drive the reaction is decreased. This decrease is also indicative of a decrease in the stability of the microstructure and one would expect the ductility to also decrease. However, this is not what is observed since TMP6 shows a higher peak ductility than TMP1.

When the area under the DSC traces of TMP1 and TMP6 are compared, it is apparent that TMP6 has the more stable microstructure and should, therefore, exhibit the greater superplastic response, which it does. Consequently, to predict the superplastic response from the DSC data one would have to say that the second endothermic peak appears to be a good indicator of the microstructural stability. However, by itself it is inconclusive and requires the additional information provided by the calculation of the area under the DSC curve to be more accurate. Although this is not exact it is a possible predictor for the expected superplastic response.

The effect of the reduction per pass on the samples' superplastic response cannot be isolated. Additionally, there is no strong evidence to support a specific reason for the actual effect. The additional uncertainty introduced when the effect of reduction per pass is compared in the short (4 minutes) reheat and the long (30 minutes) reheat

times make it even more difficult to determine a distinct effect attributable only to the reduction per pass.

3. Effect of Reheating Time (4 Min vs. 30 Min)

The results obtained from investigating the effects of the reduction per pass were not conclusive. The single, most significant variable in the thermomechanical processing identified is the amount of reheating time experienced between each warm rolling pass. In either the large reduction material (Figure 4.15) or the low reduction material (Figure 4.16), increased reheating time from 4 minutes to 30 minutes produces a very profound increase in the magnitude of the heat capacity. In each case, when the reheating time was increased the magnitude of the endothermic peak was seen to be much higher and the area under DSC traces were significantly greater. These increases indicate that the microstructures are more stable and a higher ductility is expected in either of the longer reheating time thermomechanical processes.

Increasing the reheating time between each pass caused an increase in the superplastic response of both reductions per pass schemes investigated. The magnitude of the increase in the ductility was most significant when TMP2 and TMP6 were compared.

4. Summary

A distinct effect for each of the three variables investigated could not be isolated. Increasing the final

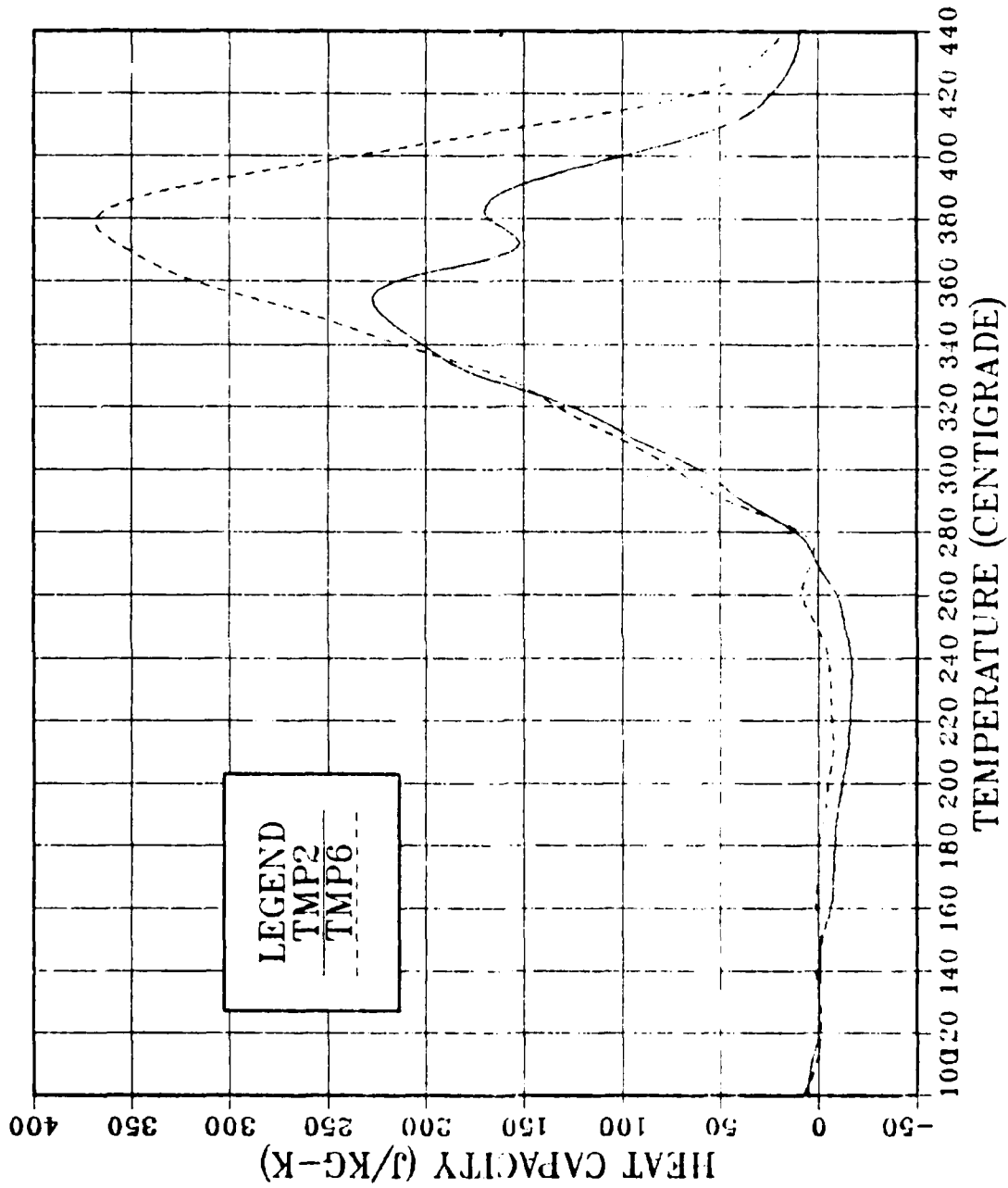


Figure 4.15 Graph of Heat Capacity vs. Temperature for Processes TMP2 and TMP6

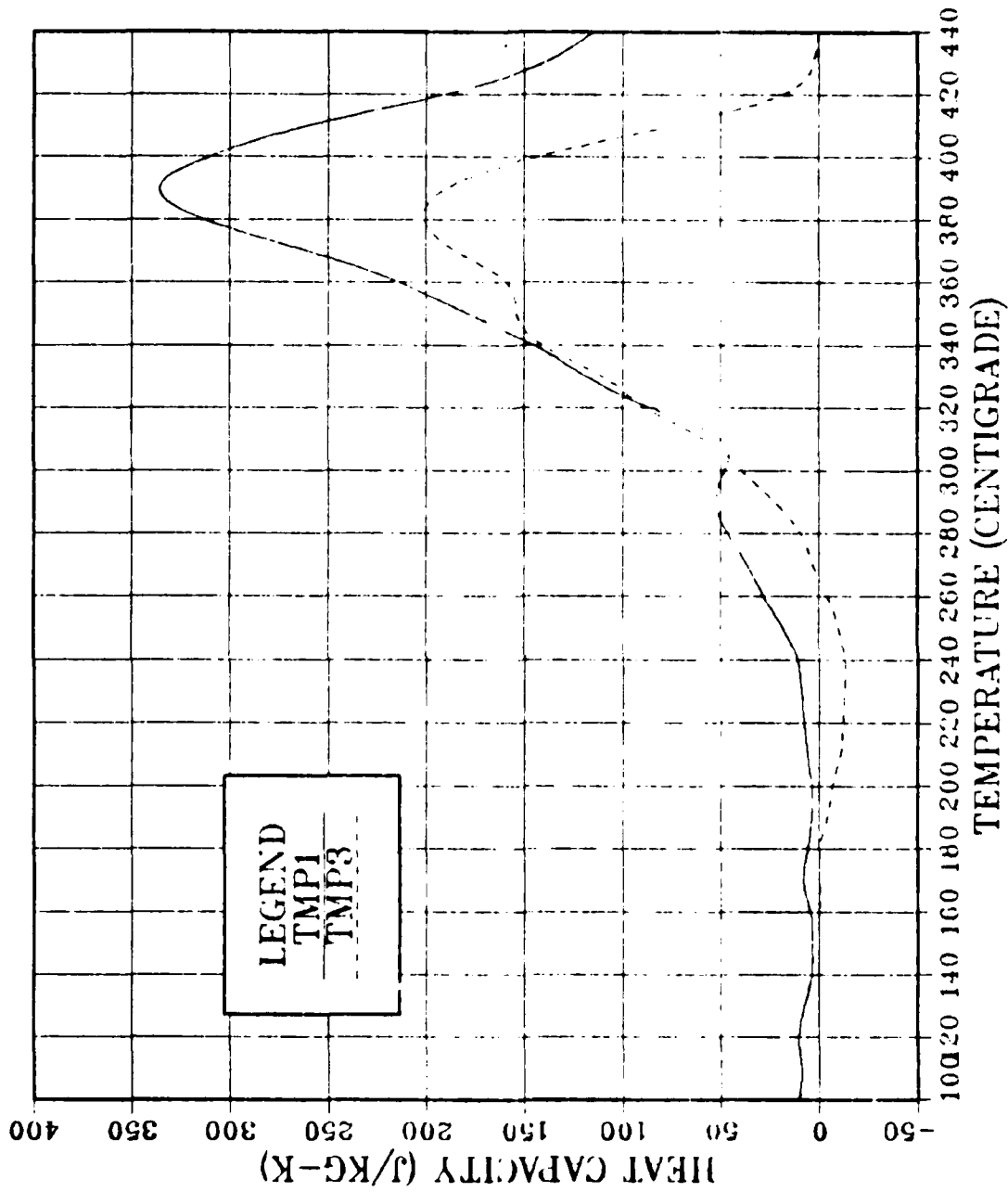


Figure 4.16 Graph of Heat Capacity vs. Temperature for Processes TMP1 and TMP3

true strain from 1.5 to 2.5 caused the ductility to increase, indicating a finer, more stable microstructure as also evidenced by the increase in energy required to cause the endothermic reaction(s) to occur. When the reduction per pass is increased the potential for superplastic response exists, but to achieve this superplasticity a concurrent increase in the reheating time between each warm rolling pass must also occur. This increase in reheating time must be long enough to allow sufficient microstructural stabilization which is seen as a removal of the exothermic reactions, i.e., by allowing time for recovery and/or recrystallization to occur, and this can also be seen in an increase in the endothermic energy detected by the DSC. The reduction per pass seems to be relatively less significant in obtaining superplastic response, but it does dictate the reheating time required between passes.

C. TRANSMISSION ELECTRON MICROSCOPY

To accurately characterize the microstructure and its evolution during heating the transmission electron microscope was employed to investigate the changes that the differential scanning calorimeter detected. The first comparison considered was between the as-rolled samples and those that had been heated to 573K (300°C) and held for 10 hours, for each of the differently processed materials.

1. As-rolled Microstructure

The microstructures for the as-rolled condition of each TMP were similar. Each process produces a highly distorted matrix containing an extremely high dislocation density. In spite of this high dislocation density one feature was identifiable in all processes, namely, a banding parallel to the rolling direction. In the absence of recrystallization one would expect grains to simply elongate, so this banding effect is not unexpected. The magnitude of the banding varied from the distinct stratification seen in TMP2, Figure 4.17a, to being just discernible in certain areas in TMP6, Figure 4.17b. This banding is accentuated in TMP2 by 'stringers' of submicron size visible at the band boundaries, whereas in TMP6 larger, more discrete β particles are observed and appear to be located adjacent to the apparent grains.

The dislocation density was sufficiently high to preclude identification of grain boundaries in the samples that had only 4 minutes per pass reheating time (TMP2, TMP3, and TMP4). Although some portions of the grain boundaries were visible, the actual grain size could not be determined. The increased reheating time between passes to 30 minutes in TMP1 and TMP6 resulted in a microstructure that showed some areas where grains could be identified (from 0.5 to 4.0 microns in size) and discrete β particles could be seen (0.5 to 1.0 μm in size) in TMP6.

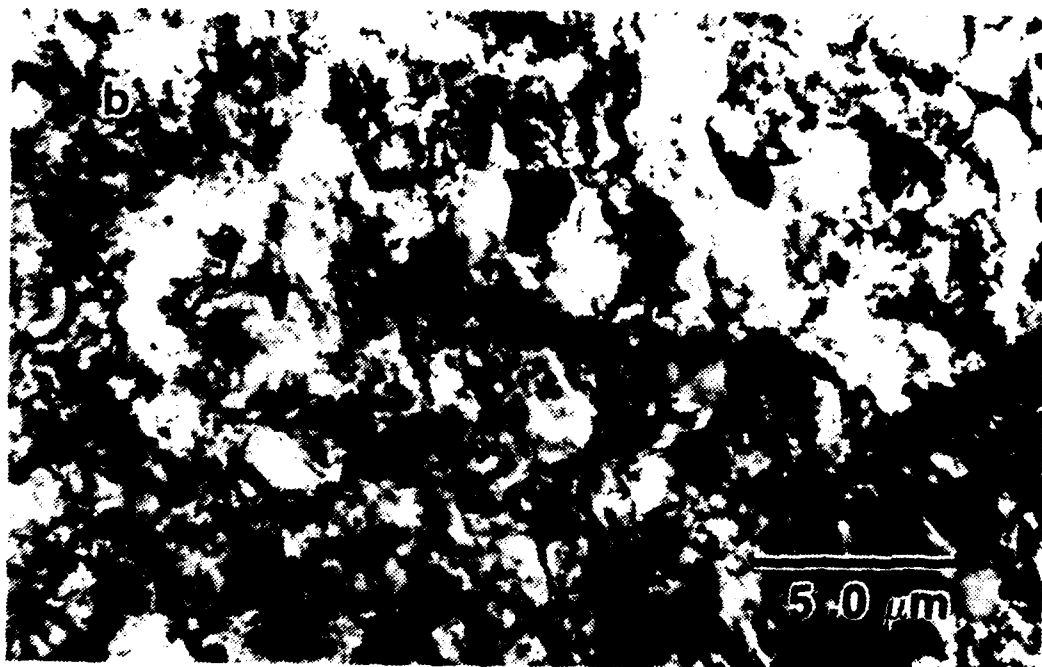
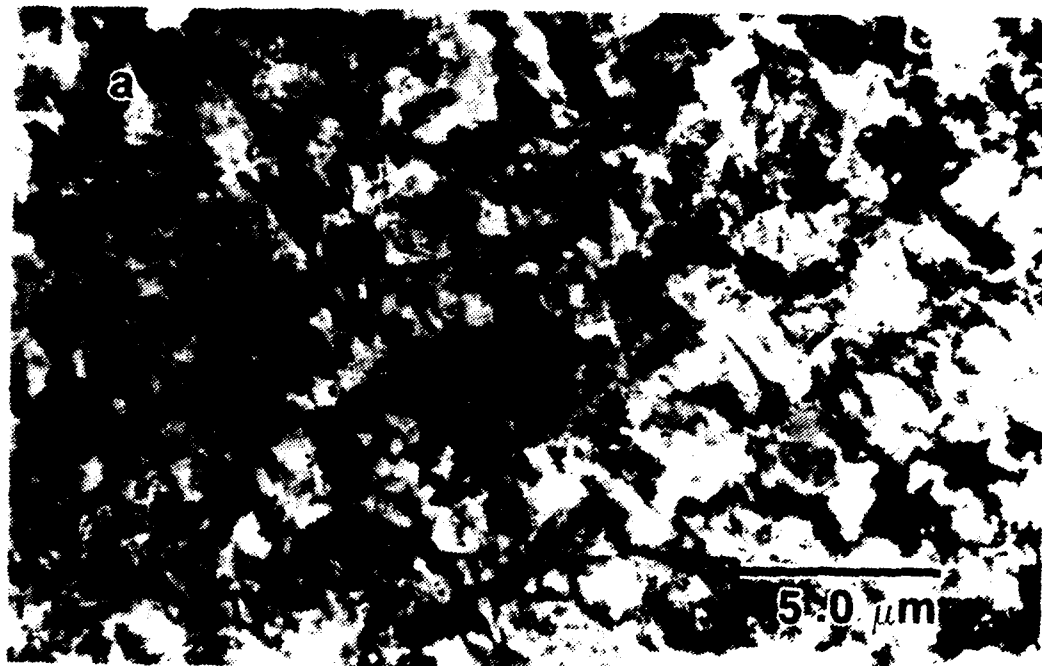


Figure 4.17 TEM Micrograph of an Al-10Mg-0.1Zr Alloy in the As-rolled Condition (a) TMP2 (b) TMP6

Such microstructure in general would not be expected to exhibit superplastic behavior, however superplastic response has been observed previously in this alloy by Hartman [Ref. 24], Berthold [Ref. 21], Klankowski [Ref. 23], Grider [Ref. 25], and Wise [Ref. 28], as well as here. Therefore there must be some point before or during the mechanical testing at which the microstructure transforms to a condition such that it can support superplastic deformation.

2. Microstructure After 10 Hour Anneal at 573K (300°C)

The samples that were heated to 573K (300°C), held for 10 hours and then cooled to room temperature, fall into two microstructural categories; small (0.5 μm to 5.0 μm) grain size and large (3 to 15 μm) grain size. The apparent small grain size was observed in TMP2, TMP3, and TMP4, as shown in Figure 4.18a, and the large grain size was found in TMP1 and TMP6, as shown in Figure 4.18b. Again, the reheating time between each rolling pass seems to be the factor that significantly affects the microstructure.

In the processes that experienced only 4 minutes reheating between passes, TMP2, TMP3, and TMP4, the small apparent grain size was not expected since these samples have undergone static annealing for 10 hours. Since dislocation structures were visible in some of these apparent grain boundaries, these boundaries were examined further. In Figure 4.19 the dark field micrograph of the

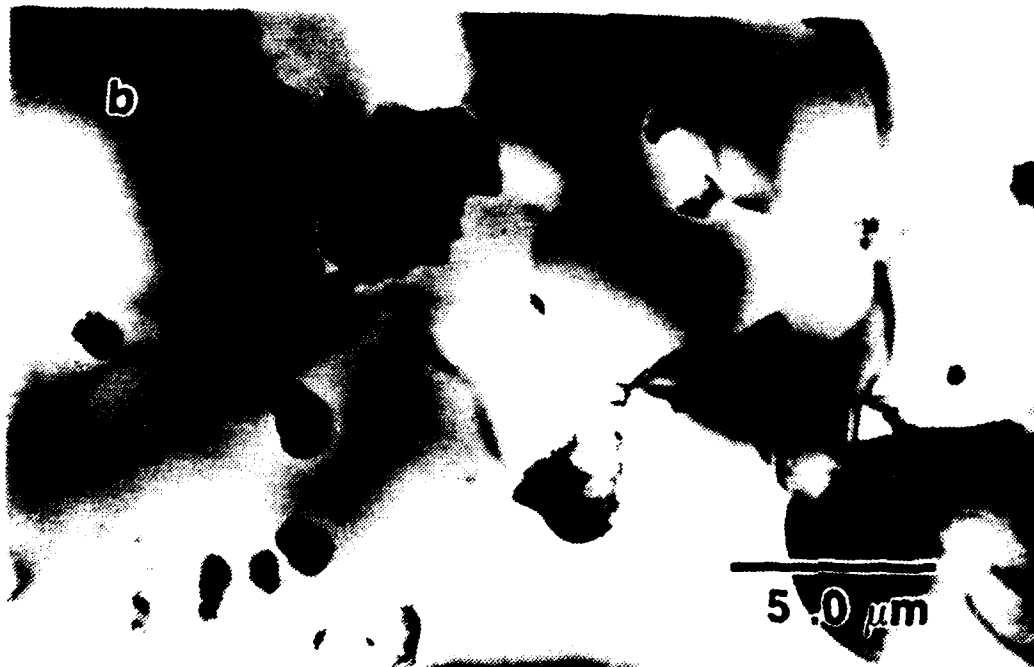


Figure 4.18 TEM Micrograph of an Al-10Mg-0.1Zr Alloy
in the 10 Hour Annealed Condition
(a) TMP2 (b) TMP6

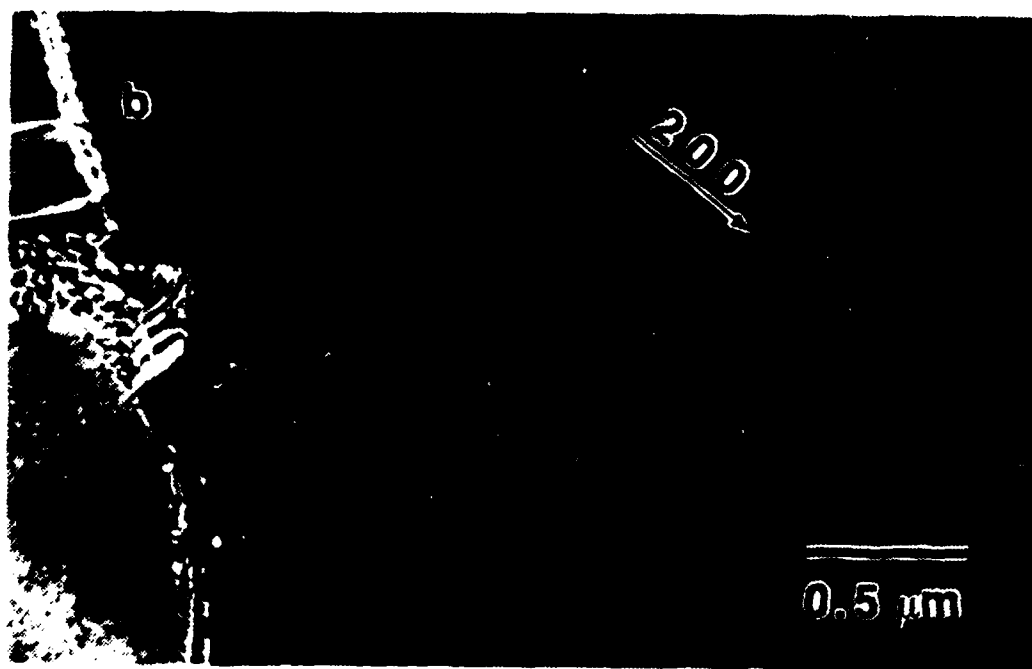
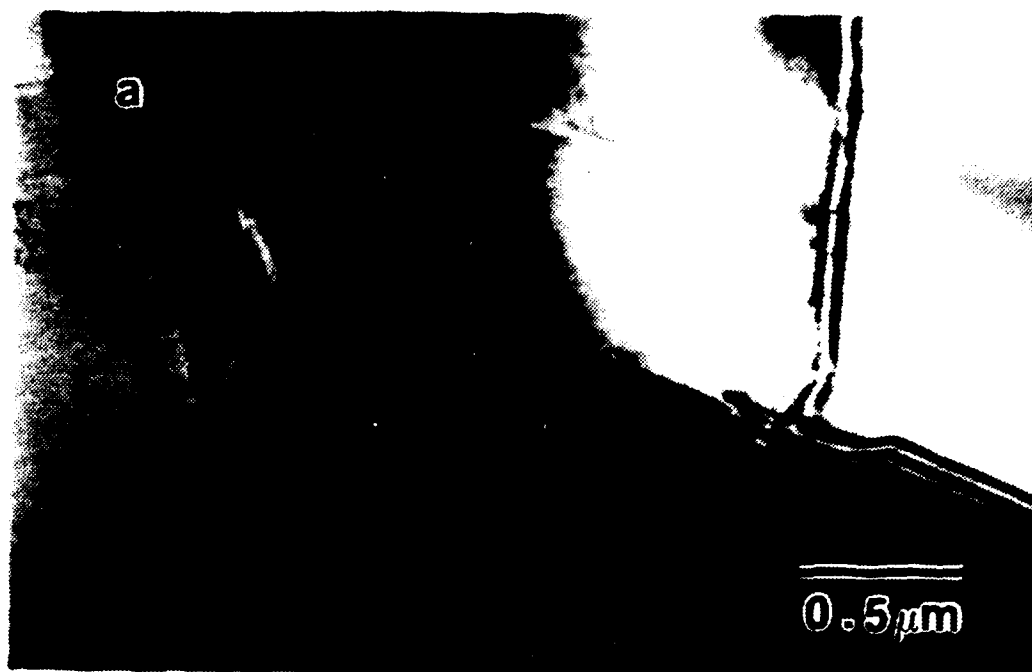


Figure 4.19 TEM Micrograph of an Al-10Mg-0.1Zr Alloy Processed by TMP2 and Annealed for 10 Hours (a) Bright Field (b) Dark Field

observed apparent grain boundary images the dislocations, indicative of a subgrain boundary. This is typical of the apparent grain boundaries throughout the TMP2 sample. Consequently, the observed boundaries are judged to be subgrain boundaries and the observed substructure is simply contained within a relatively large grain.

An additional similarity observed between the three short reheating time samples was that there were regions throughout the microstructure rich in precipitates and other regions that were lean in precipitates. In each of these short reheating time samples the β -rich regions possessed an extremely fine structure with a spacing between boundaries of 0.25 to 1.5 μm where in the β -lean regions the spacing was of the order of 2 to 5 μm .

The microstructure observed in the long (30 minute) reheating time samples, TMP1 and TMP6, was that expected of an annealed material. The size of the grains in the TMP1 sample was, in general, larger (5 to 15 μm) than those in the TMP6 sample (3 to 8 μm), which may reflect on the total time at temperature during processing being twice as long in TMP1 as in TMP6. In each case a distinct absence of dislocations in an equiaxed grain structure was observed, indicating that recrystallization has occurred. Within some of the grains a finer substructure (1 μm in size) was observed. The dark field micrographs, Figures 4.20 and 4.21, show that such boundaries are subgrain boundaries.

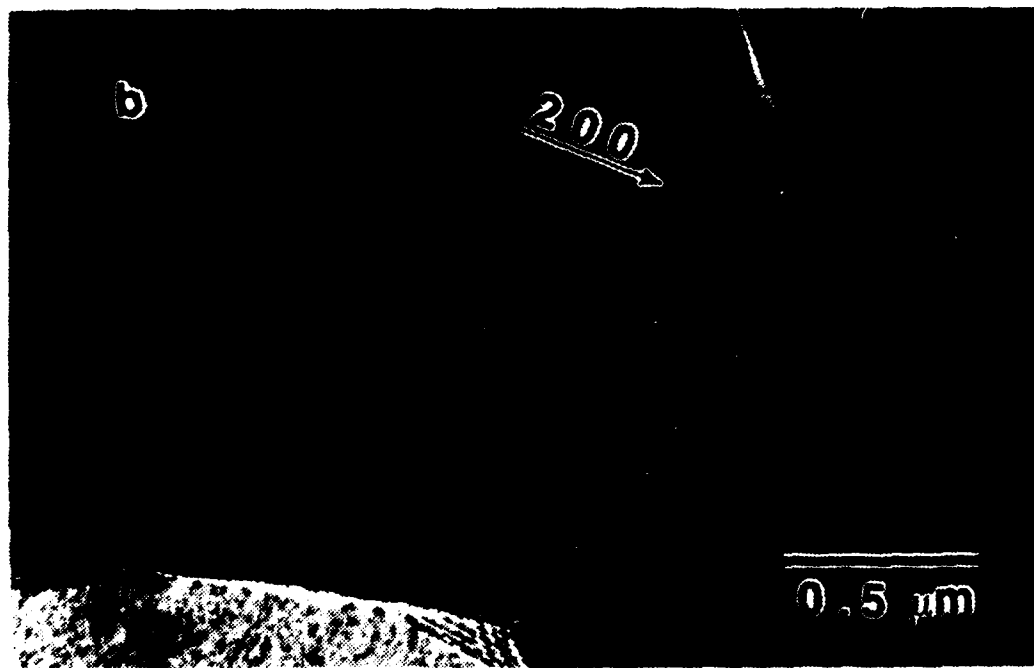
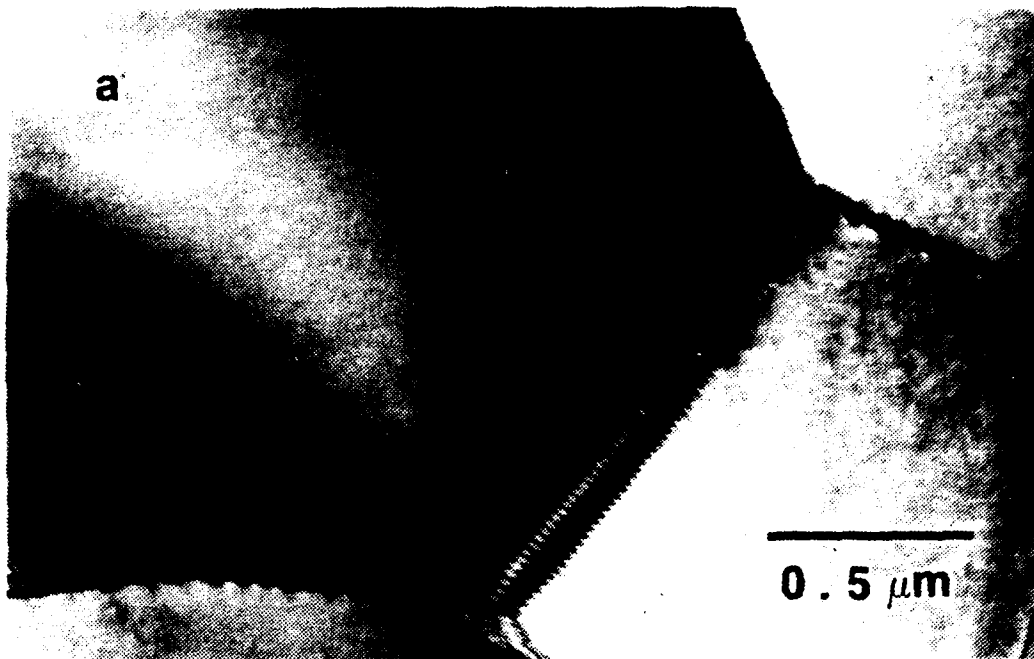


Figure 4.20 TEM Micrograph of an Al-10Mg-0.1Zr Alloy
Processed by TMP6 and Annealed for 10 Hours
(a) Bright Field (b) Dark Field

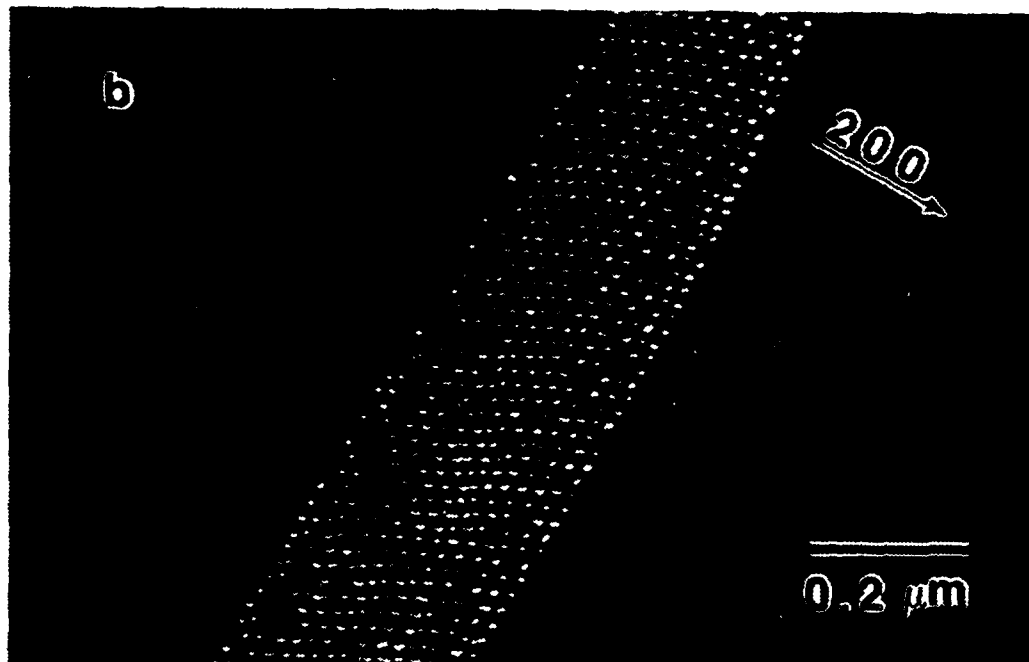
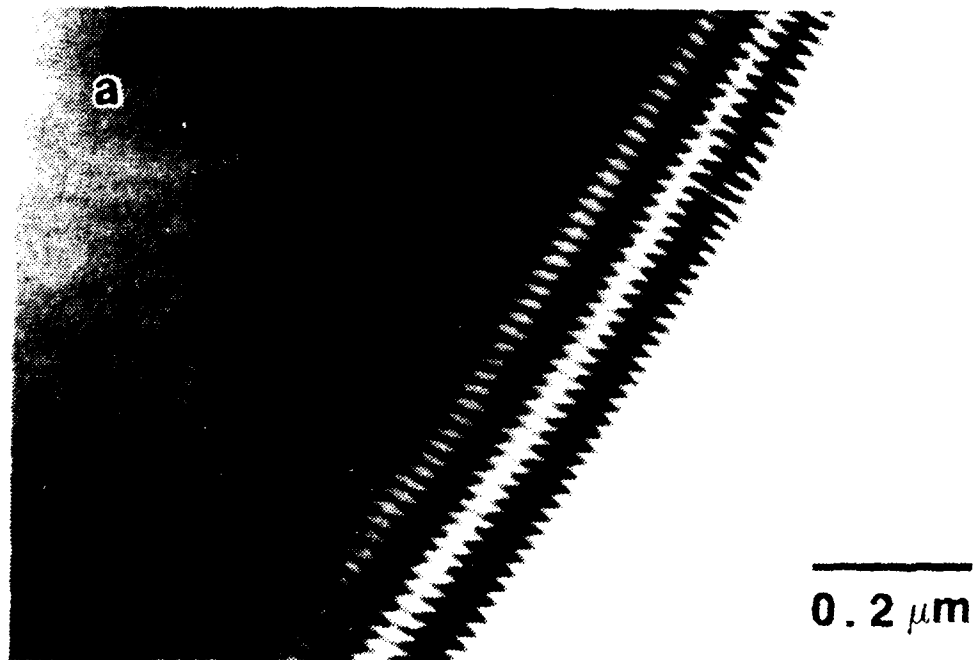


Figure 4.21 TEM Micrograph of an Al-10 Mg-0.1Zr Alloy
Processed by TMP6 and Annealed for 10 Hours
(a) Bright Field (b) Dark Field

The distribution of the β phase in TMP1 and TMP6 was essentially uniform and no stringers were found. There was a trimodal size distribution of particles found in specific microstructural locations. Precipitates of 0.2 to 0.5 μm size were found in the grain interiors, 0.75 to 1.5 μm along the grain boundaries, and 2 μm sized β particles at grain boundary triple points. The largest particles, located at grain triple points, appeared faceted and exhibited heavy faulting.

3. Comparison of As-rolled and the 10 Hour Anneal Samples

A comparison of the as-rolled material to that rolled and then annealed for 10 hours at 573K (300°C) shows significant changes occur upon annealing. These changes warrant further investigation into the actual microstructural changes occurring by comparing the microstructures at shorter annealing times. The majority of previous work completed more nearly approximates to TMP2 than any other thermomechanical process. Couple this fact with the observation that reheating time between each pass is the most significant variable indicates that an in-depth comparison of TMP2 and TMP6 could potentially lead to a better understanding of the evolution of the microstructure.

4. TMP2 and TMP6: Annealed One Hour

The microstructures for the samples that were processed by TMP2 and TMP6, heated to 573K (300°C), and held for one hour are shown in Figures 4.22a and 4.22b. When

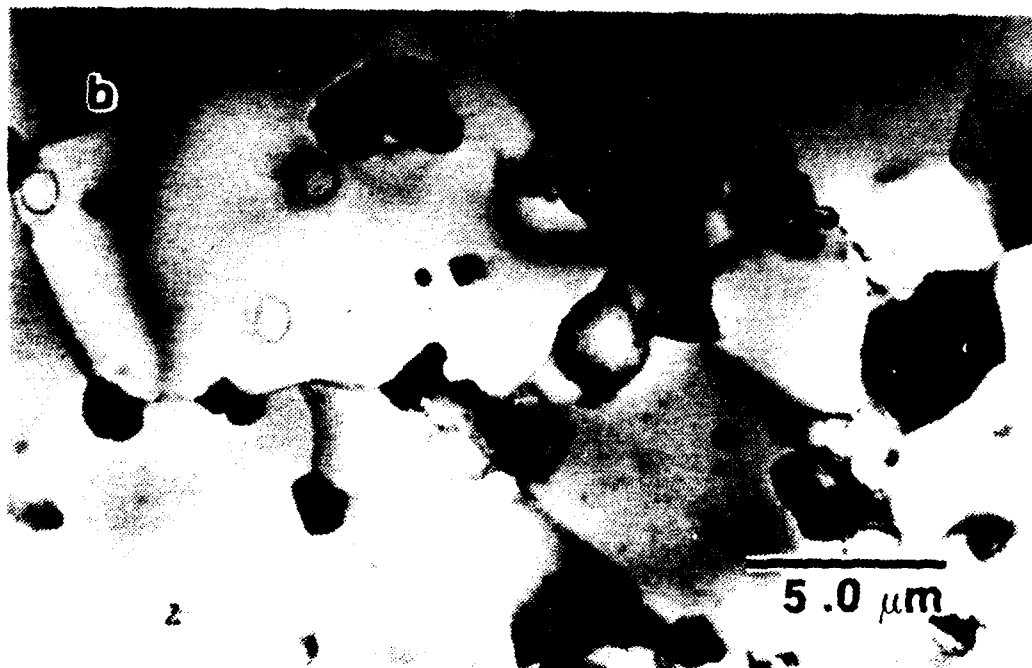


Figure 4.22 TEM Micrograph of an Al-10Mg-0.1Zr Alloy
in the 1 Hour Annealed Condition
(a) TMP2 (b) TMP6

these microstructures are compared to the samples that have been annealed for 10 hours at 573K (300°C) there is little discernible difference. Other than very slight grain growth, it may be inferred that the microstructure of the samples that were annealed for one hour at 573K (300°C) essentially is a stable structure.

To verify this microstructural stability a sample of the TMP2 sample was annealed for 42 hours at 573K (300°C). Figure 4.23 shows that even after 42 hours the microstructural changes basically are insignificant. This indicates rapid microstructural change initially (up to 1 hour) followed by little change thereafter.



Figure 4.23 TEM Micrograph of an Al-10Mg-0.1Zr Alloy Processed by TMP2 and Annealed for 42 Hours

5. Grip Section Microstructure

To investigate the microstructure during the first hour at 573K (300°C) samples were taken from the grip sections of tensile test specimens tested at a strain rate of 1.67×10^{-1} 1/sec (this strain rate was chosen because deformation to failure occurred within about 15 seconds). The heating of the test specimen from room temperature to the test temperature, allowing for equilibration of the furnace, takes 40 to 55 minutes. Consequently, after the sample has failed it has been at 573K (300°C) for less than an hour.

In these samples similarities between the microstructures has been noted; the substructure was 0.25 to $2.0 \mu\text{m}$ in size; the size of the β precipitates is less than or equal to $1.0 \mu\text{m}$, and there are β -rich and β -lean regions in each sample. Figure 4.24 shows that the microstructure of the TMP2 sample has the same substructure size seen in the 1 hour or 10 hour annealed samples, but the TMP6 sample has larger grains (up to about $5.0 \mu\text{m}$). It is quite apparent that there must be some microstructural coarsening occurring in TMP2 even though this investigation was unable to determine the actual grain size of the material that underwent TMP2 since the TMP6 microstructure shows that grain growth is occurring.

Comparing these microstructures to those of the one hour anneal, Figure 4.22, shows that the TMP sample

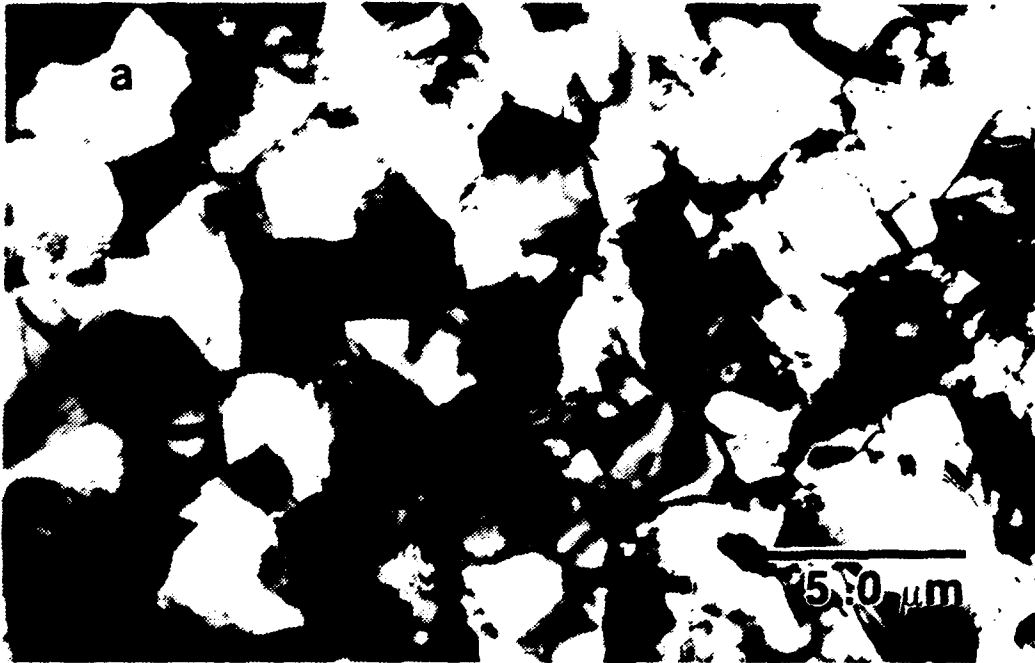


Figure 4.24 TEM Micrograph of an Al-10Mg-0.1Zr from the Grip Section of a Tensile Test Sample (a) TMP2) (b) TMP6

apparently undergoes no microstructural change whereas the TMP6 sample may. The apparent change of the microstructure of the TMP6 sample from the grip section with respect to that of the one hour static anneal cannot be accurately accounted for. This difference may be due to stress-induced effects in the grip section, the difficulty arises since the effects of the stress experienced by the grip section sample cannot be isolated from the thermal effects. The comparison supports the hypothesis that microstructural evolution occurs, but one cannot accurately distinguish between the thermally induced and stress induced effects.

V. CONCLUSIONS AND RECOMMENDATIONS

A. CONCLUSIONS

The following conclusions are drawn from the data and observations made during this research.

1. When the warm rolling total true strain is increased from 1.5 (TMP4 and TMP5) to 2.5 (TMP2 and TMP3) higher ductilities are observed.
2. The increased ductility with increased total true strain is much more pronounced and is observed to be of higher values in the lightly reduced material (TMP3) than in the heavily reduced material (TMP2).
3. The increase in total true strain weakens the material.
4. Increasing the reheating time between passes from 4 minutes to 30 minutes results in higher peak ductilities and a wider range of strain rates over which superplastic response is observed.
5. The increase in peak ductility caused by the increase in reheating time and the range of strain rates over which superplasticity is observed is significantly more pronounced in the heavily reduced material than in the lightly reduced material.
6. The effect of the amount of reduction per pass is an intricate function of total true strain and reheat time between passes.
7. The Differential Scanning Calorimeter shows that the beta precipitate resulting from deformation processing is different from the thermally induced beta precipitate observed in a fully recrystallized material.
8. Differential Scanning Calorimetry results indicate that ductilities are an intricate function of the three variables investigated, but can predict which process will be more ductile when the relative position of the second endothermic peak and the area under the DSC traces (endothermic energy) are compared.

9. Transmission Electron Microscopy reveals that for the large reduction per pass materials the short reheat time between passes results in a much finer substructure. The observed higher ductility in the coarser substructure (TMP6) occurs because the fine substructure of TMP2 is subgrains whose misorientation is not sufficient to support boundary sliding.
10. The Transmission Electron Microscope shows that the grain sizes of the two longer reheating time samples (TMP1 and TMP6) are quite similar and thus reveals a reason for the coincidental similarity in observed ductility.
11. The ability to obtain superplastic response is critically dependent upon the thermomechanical process used. The key variables are the final true strain and the reheat time between passes. When the reheat time between passes is correctly chosen an increase in final true strain results in significant increases in ductility.

B. RECOMMENDATIONS

The following recommendations are presented for consideration for further study.

1. Conduct a similar series of experiments with a higher reduction per pass to verify this variable's effect.
2. Using TMP1 and TMP6 as base lines conduct similar experiments for longer and shorter reheat times to accurately determine the optimum process variables.
3. With the large and small reduction per pass identified conduct experiments to a final strain of 3.0.
4. Utilize the slower scan rates, 20 K/min and 10 K/min, on the differential scanning calorimeter to determine if the DSC traces for TMP2 and TMP3 are actually a combination of two distinct transitions.
5. Reduce and analyze the data available from the differential scanning calorimetry traces produced in this research for the ramp to 573K and hold for 0, 0.1, 1.0 and 10 hours.
6. Conduct tension testing on this alloy processed according to the schedule used in this research, but stop the test at various increments of ductility

(100%, 200%, etc.) and investigate the microstructural evolution that occurs during the mechanical testing in the transmission electron microscope.

APPENDIX A

COMPUTER PROGRAM

```
10 INPUT "WHAT FILENAME.<FT> DO YOU WISH TO USE ";D$
20 INPUT "SAMPLE ID..",ID$
30 INPUT "SCALE FACTOR..",SCALE
40 INPUT "CROSSECTIONAL AREA CU. IN..",AO
50 INPUT "MAGNIFICATION RATIO..",MAG
60 OPEN "O",#1,D$
70 INPUT "ENTER THE LOAD,LBF..",F
80 INPUT "ENTER X MEASURE FROM CHART,IN..",DELX
90 S=F/AO
100 DEL=(DELX*SCALE)/MAG
110 E=DELX/0.5
120 SIGMA=S*(1+E)
130 EPSILON=LOG(1+E)
140 WRITE #1,F,DELX,S,E,SIGMA,EPSILON
150 INPUT "HIT RETURN TO CONT.,N NEW SPECIMEN, OR Q..",
ANS$
160 IF ANS$="" GOTO 70
170 IF ANS$="N" THEN CLOSE #1:CLS:GOTO 10
180 IF ANS$="Q" THEN CLOSE #1:GOTO 190
190 END
```

APPENDIX B

STRESS VS. STRAIN GRAPHS

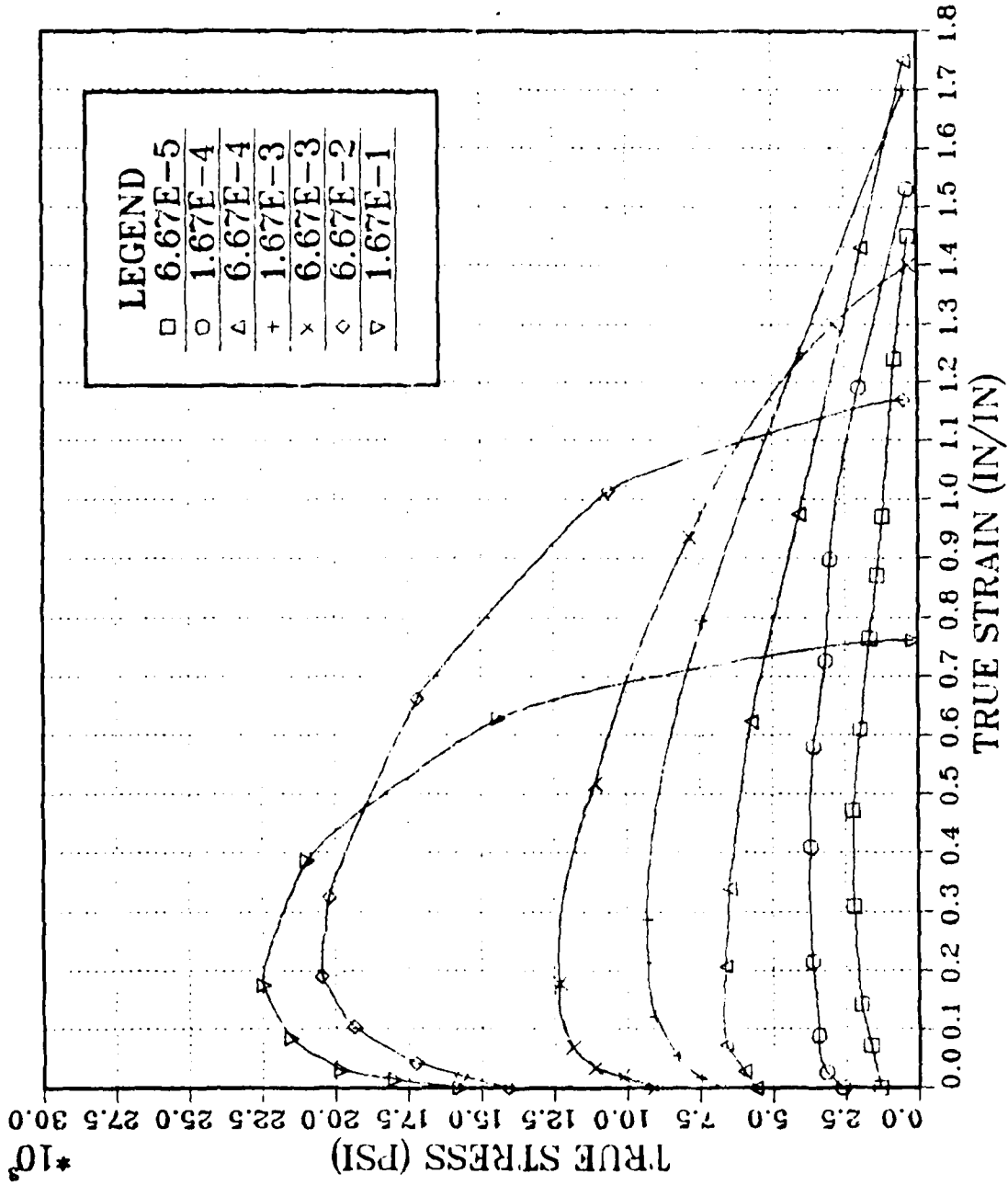


Figure B.1 True Stress vs. True Strain Plot for Tensile Testing Conducted at 300°C for an Al-10Mg-0.1Zr Alloy. The Specimen was Heat Treated and Upset Forged as Described in This Work and Warm Rolled Using Schedule TMP1 Described in Table II

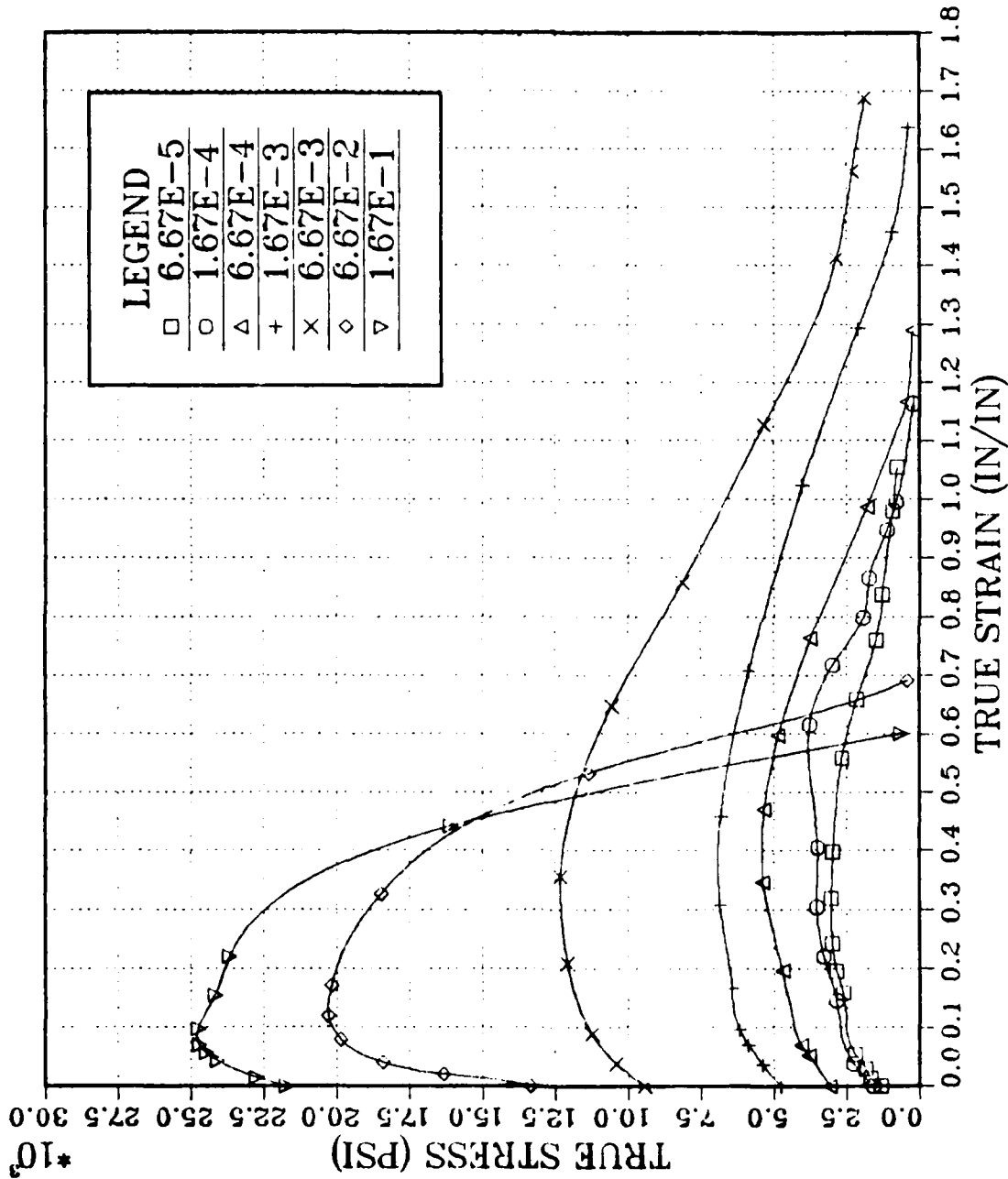


Figure B.2 True Stress vs. True Strain Plot for Tensile Testing Conducted at 300°C for an Al-10Mg-0.1Zr Alloy. The Specimen was Heat Treated and Upset Forged as Described in This Work and Warm Rolled Using Schedule TMP3 Described in Table II

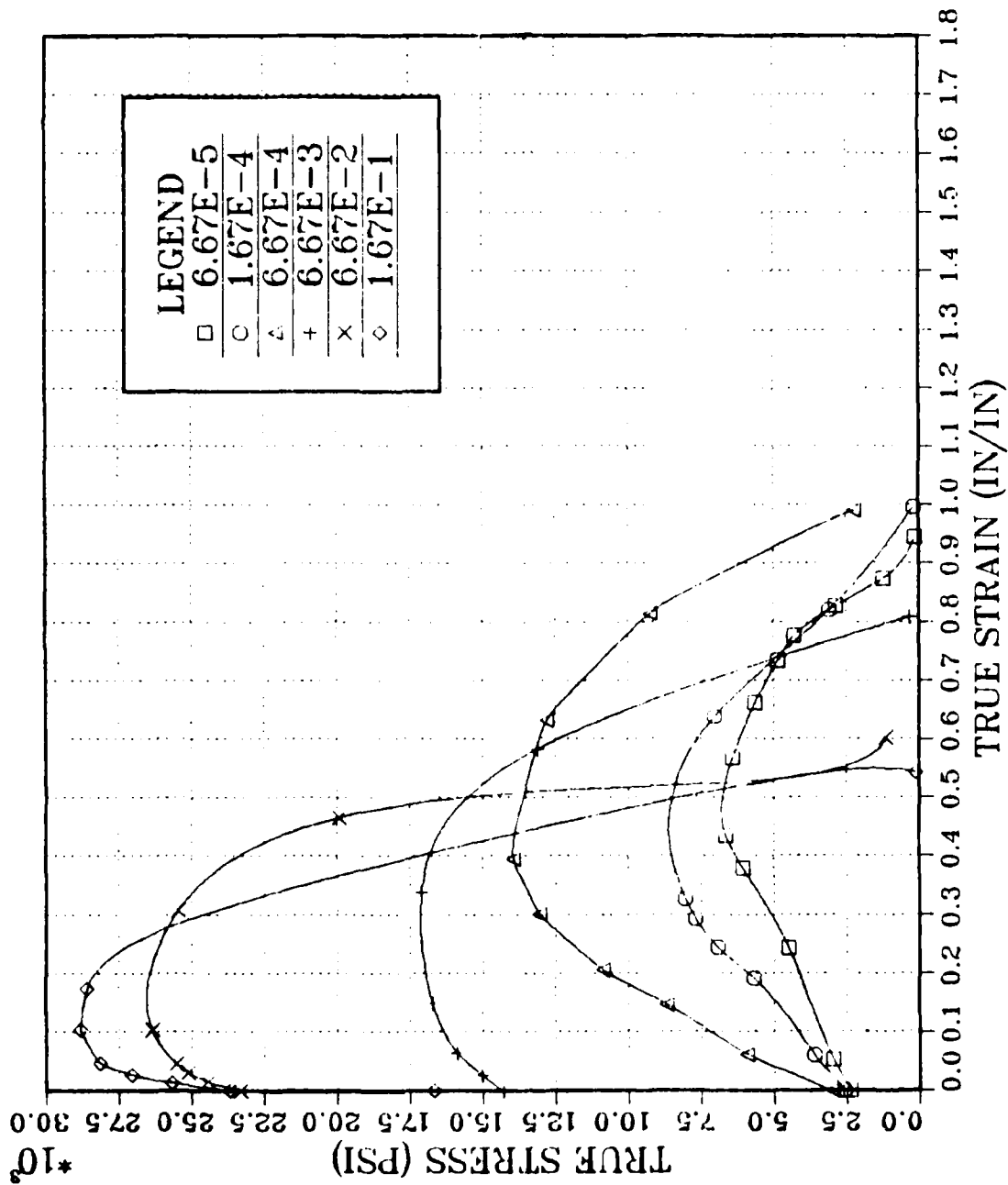


Figure B.3 True Stress vs. True Strain Plot for Tensile Testing Conducted at 300°C for an Al-10Mg-0.1Zr Alloy. The Specimen was Heat Treated and Upset Forged as Described in This Work and Warm Rolled Using Schedule TMP4 Described in Table II

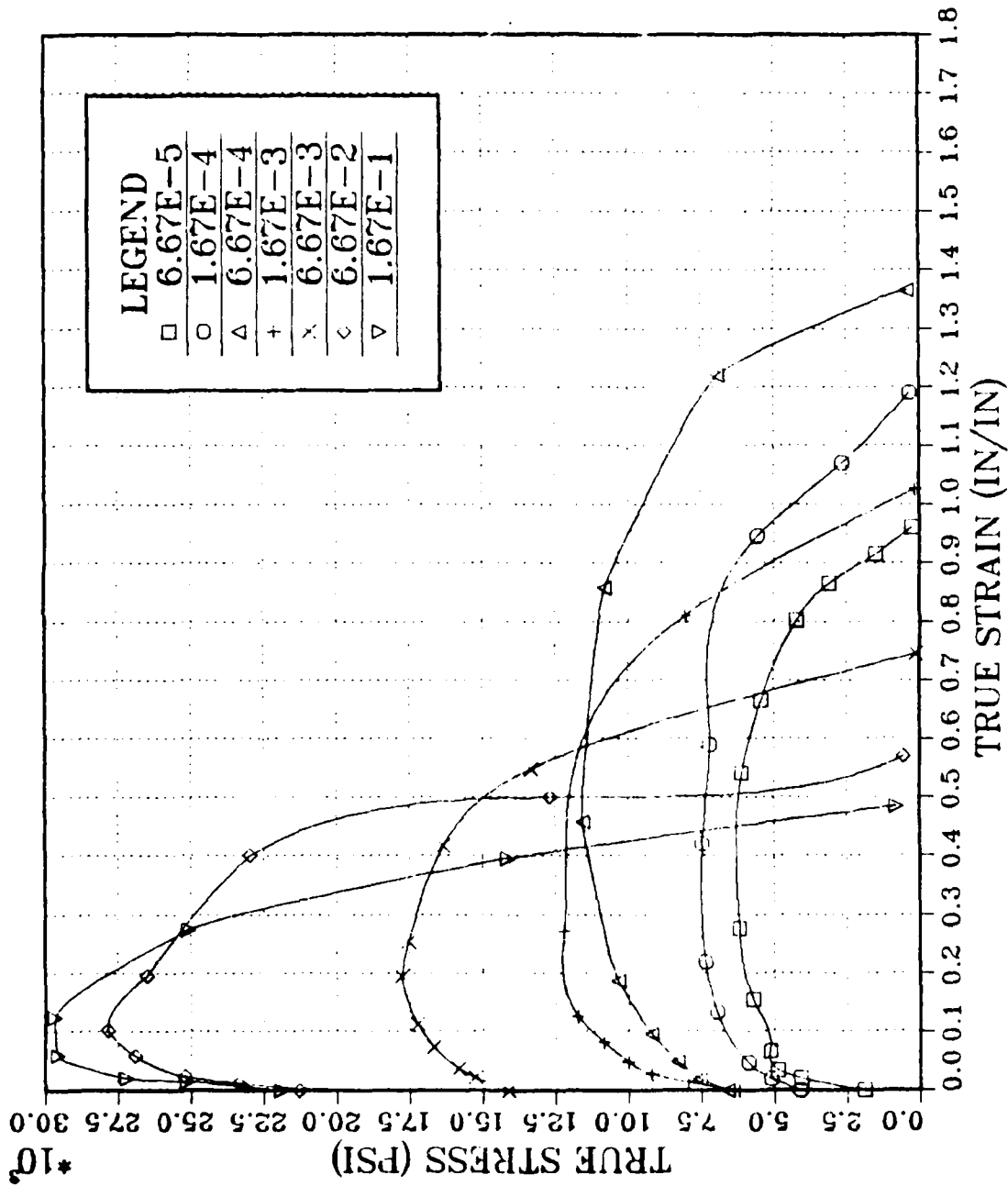


Figure B.4 True Stress vs. True Strain Plot for Tensile Testing Conducted at 300°C for an Al-10Mg-0.1Zr Alloy. The Specimen was Heat Treated and Upset Forged as Described in This Work and Warm Rolled Using Schedule TMP5 Described in Table II

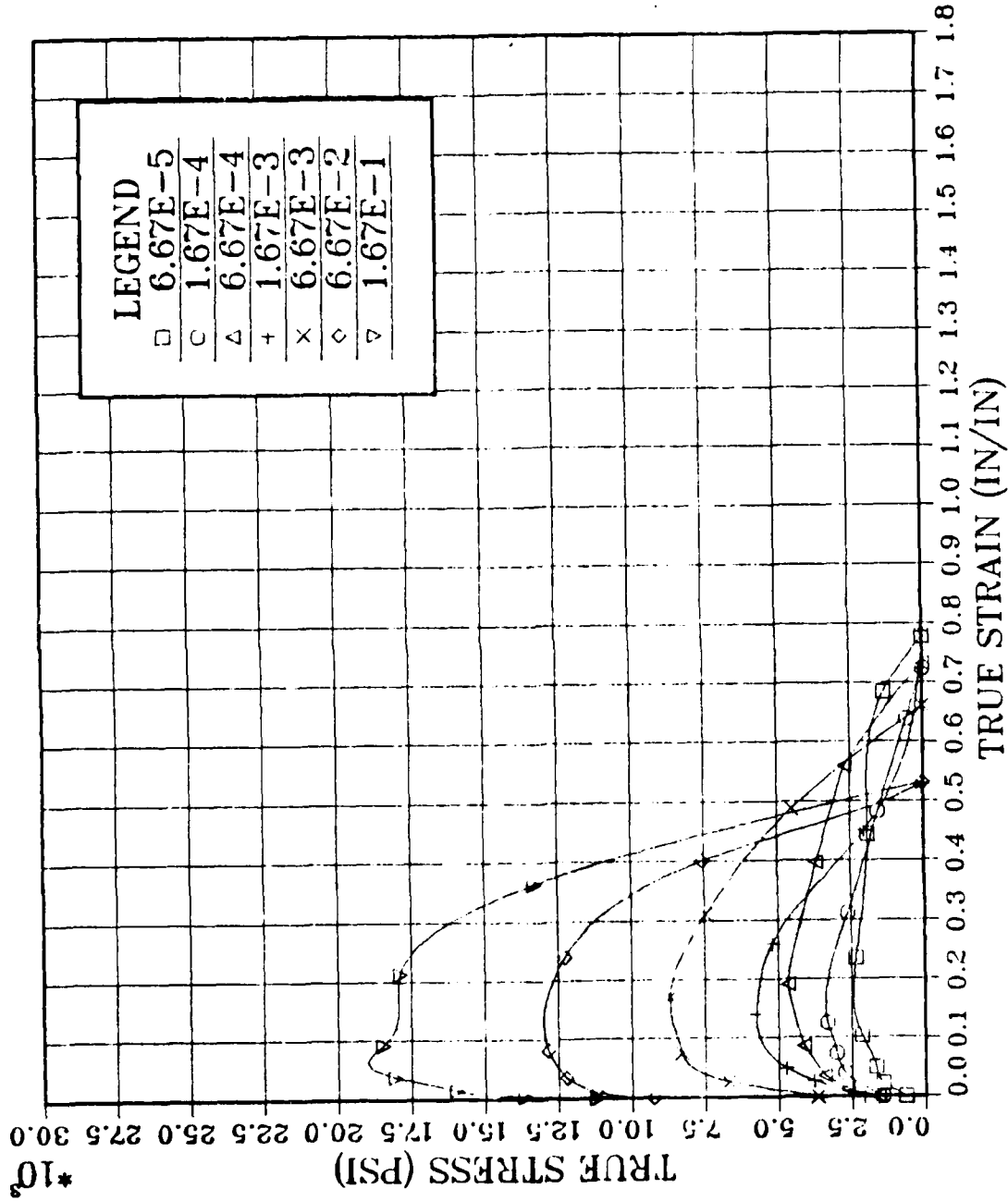


Figure B.5 True Stress vs. True Strain Plot for Tensile Testing Conducted at 300°C for an Al-10Mg-0.1Zr Alloy. The Specimen was Heat Treated and Upset Forged as Described in This Work and Warm Rolled Using Schedule TMP6 Described in Table II

APPENDIX C

HEAT CAPACITY VS. TEMPERATURE GRAPHS OF DSC DATA

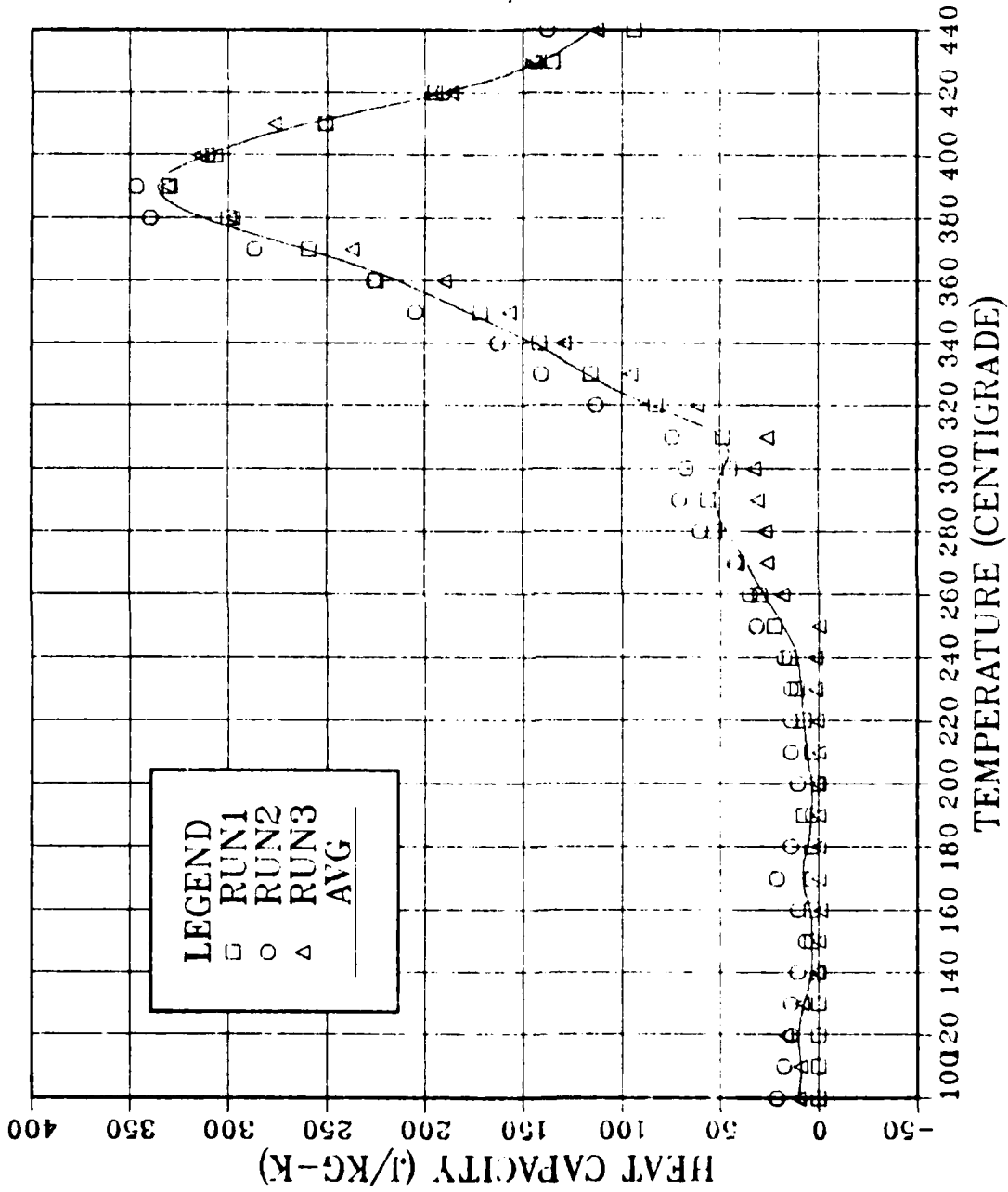


Figure C.1 Plot of Heat Capacity vs. Temperature, Raw Data, for Each of the Three DSC Runs, Plus the Average for TmP1

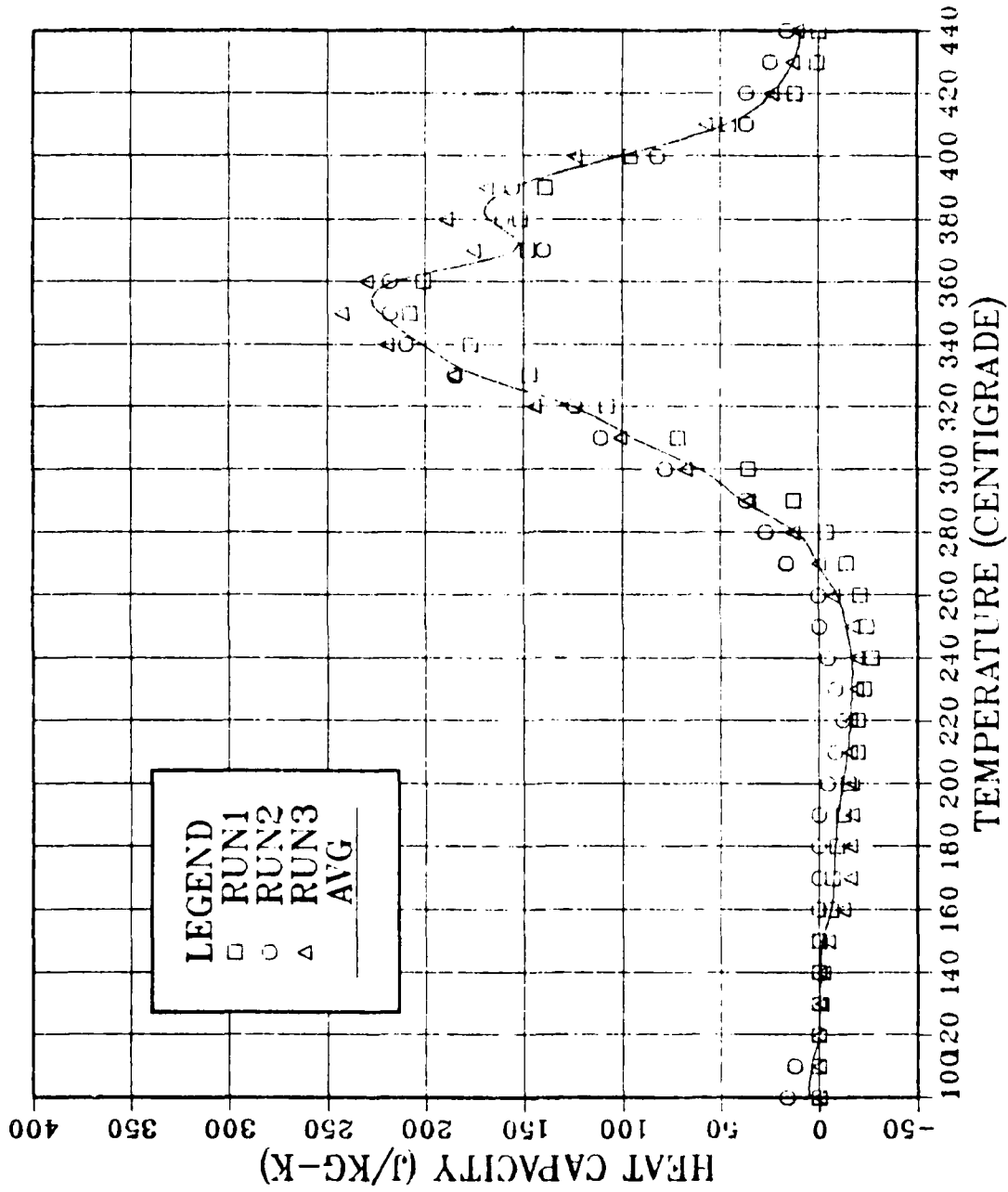


Figure C.2 Plot of Heat Capacity vs. Temperature, Raw Data, for Each of the Three DSC Runs, Plus the Average for TMP2

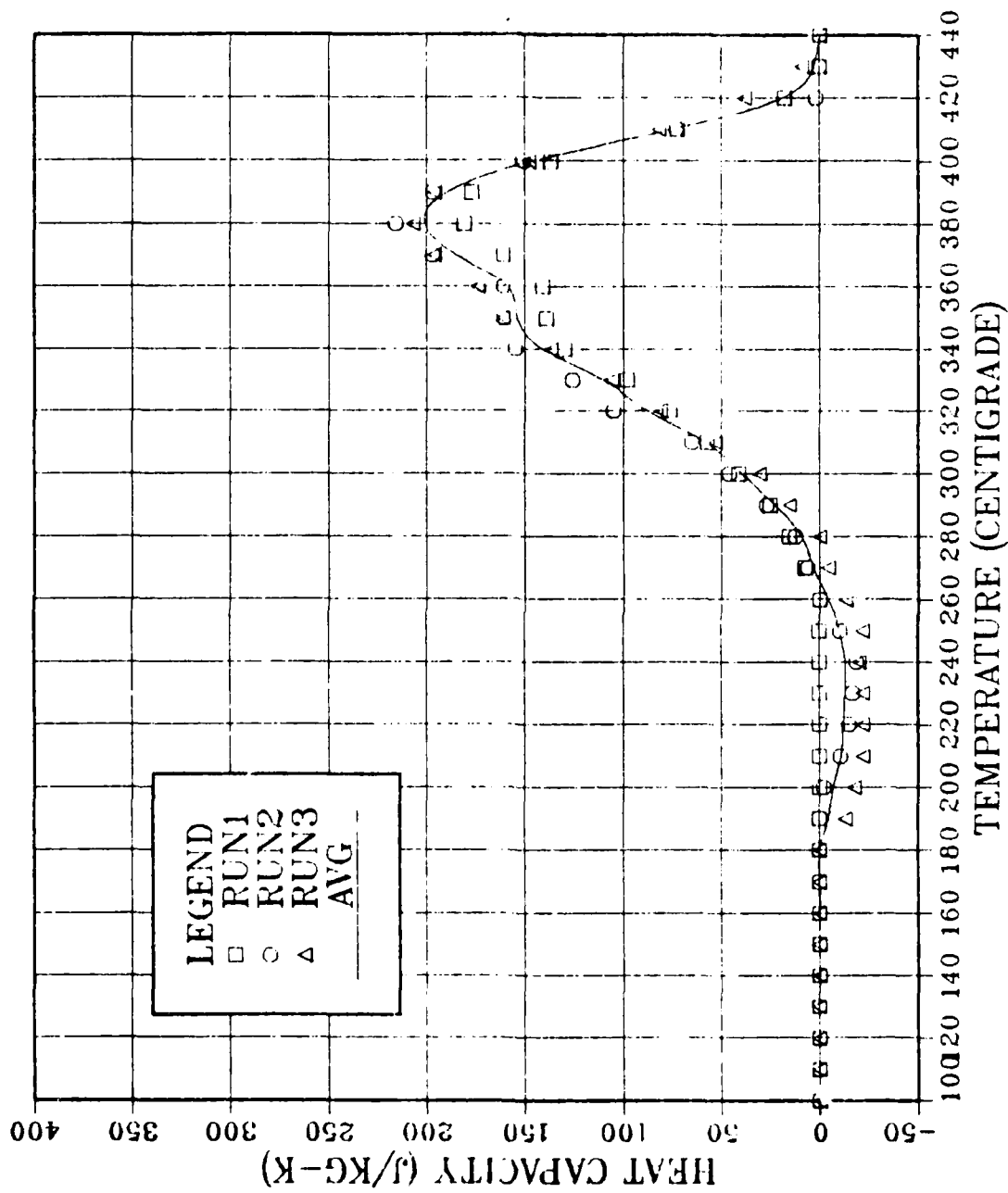


Figure C.3 Plot of Heat Capacity vs. Temperature, Raw Data, for Each of the Three DSC Runs, Plus the Average for TMP3

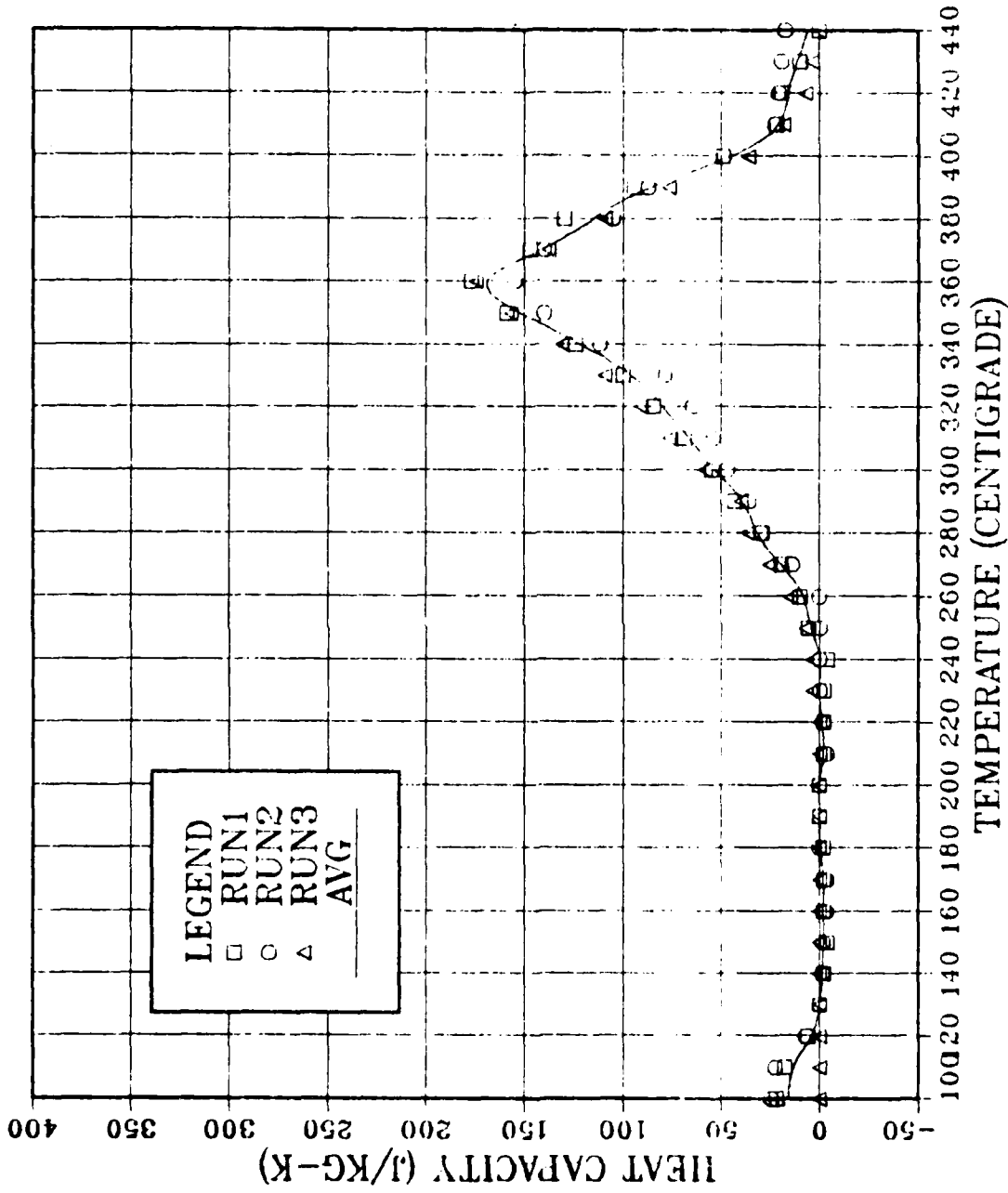


Figure C.4 Plot of Heat Capacity vs. Temperature, Raw Data, for Each of the Three DSC Runs, Plus the Average for TMP4

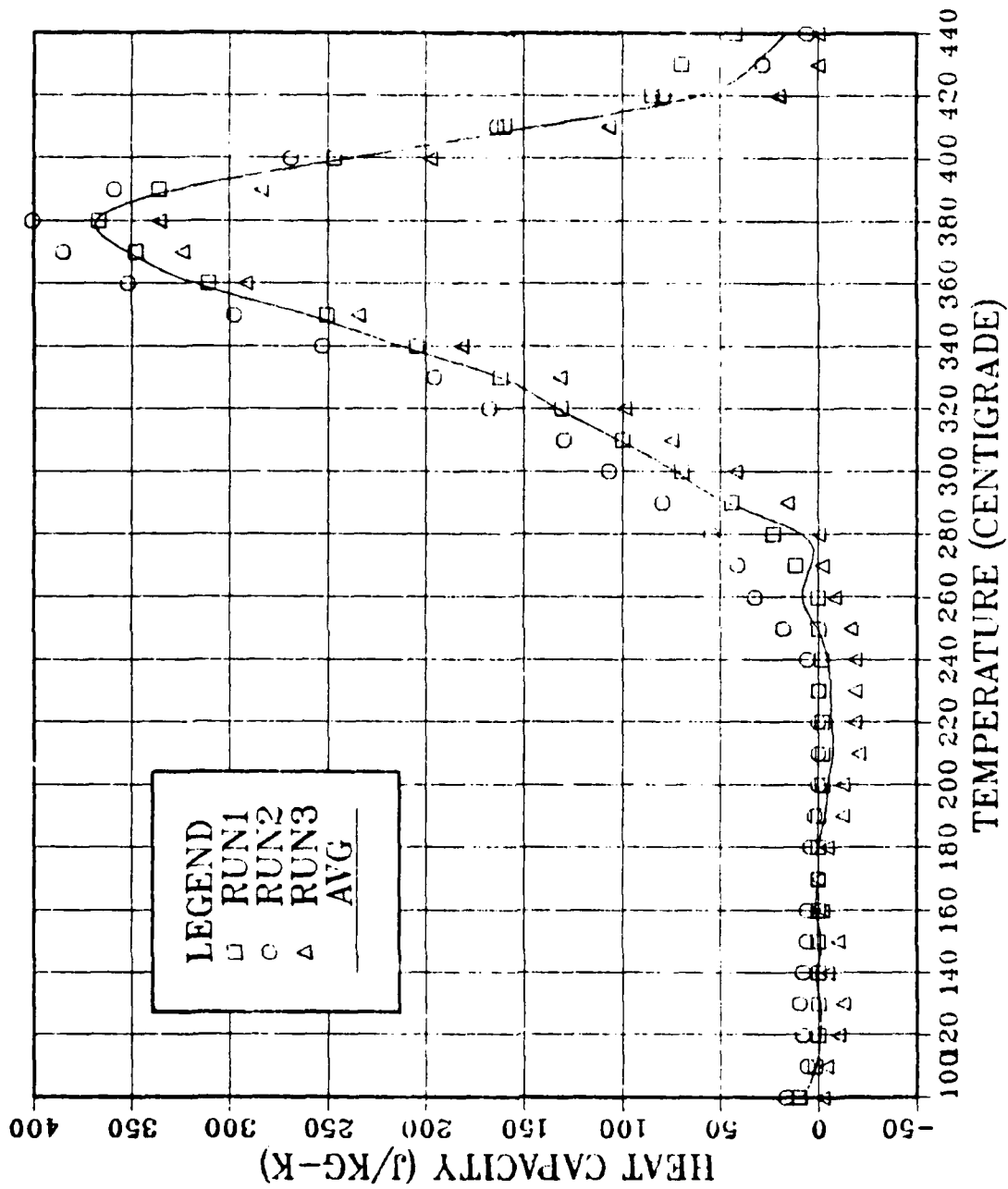


Figure C.5 Plot of Heat Capacity vs. Temperature, Raw Data, for Each of the Three DSC Runs, Plus the Average for TMP6

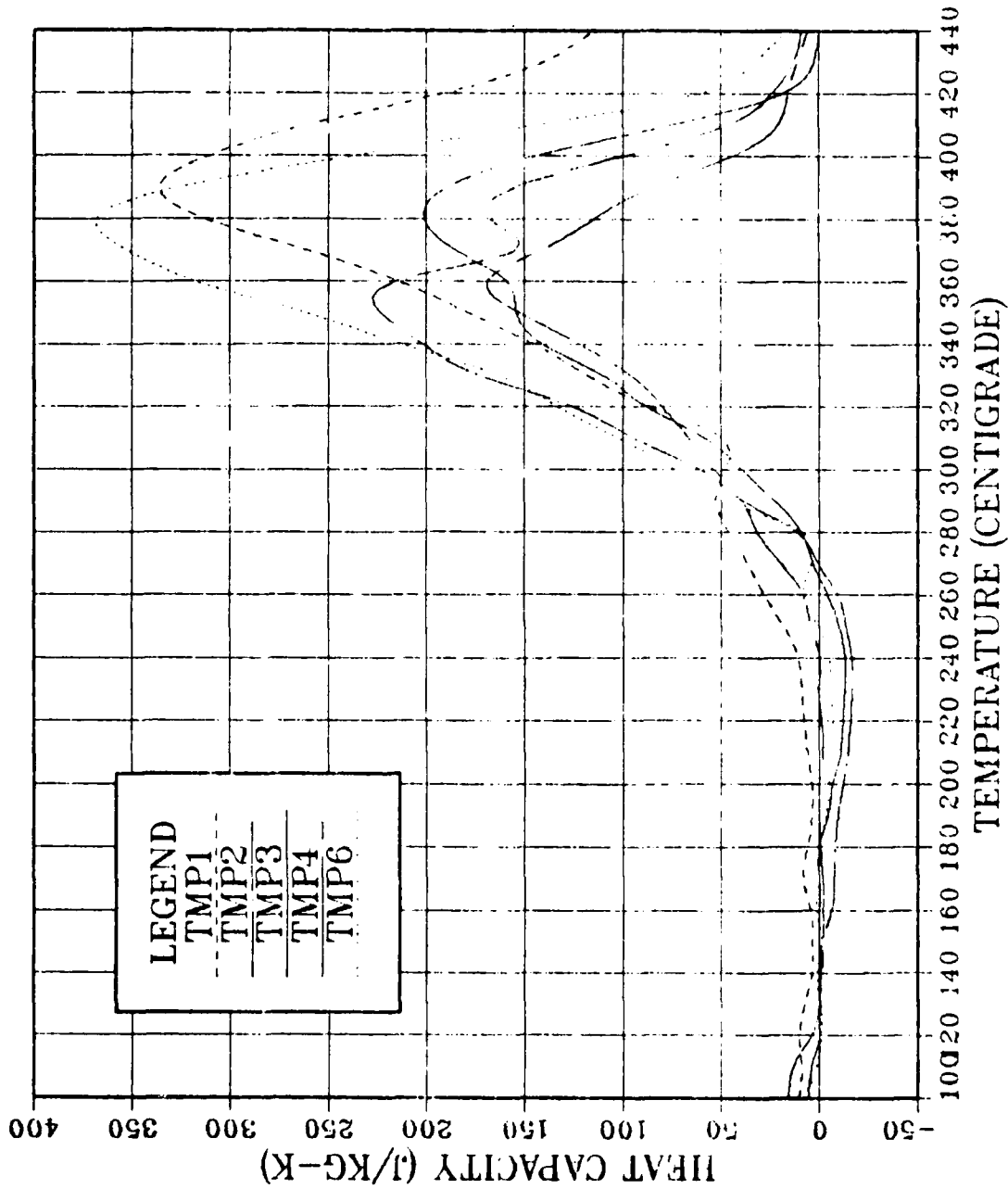


Figure C.6 Average Heat Capacity vs. Temperature Plots for All TMPs Investigated by DSC

LIST OF REFERENCES

1. Johnson, R.H., "Superplasticity," Metallurgical Reviews, V. 15, Review 146, pp. 115-134, 1970.
2. Underwood, E.E., "A Review of Superplasticity and Related Phenomena," Journal of Metals, pp. 914-919, December 1962.
3. Meyers, M.A. and Chawla, K.K., Mechanical Metallurgy, pp. 383-393, Prentice-Hall, 1984.
4. Dieter, G.E., Mechanical Metallurgy, McGraw-Hill, 1976.
5. Askeland, D.R., The Science and Engineering of Materials, Brooks/Cole Engineering Division, a division of Wadsworth, Inc., 1984.
6. Fink, W.L., et al., Physical Metallurgy of Aluminum Alloys, American Society for Metals, 1949.
7. Mondolfo, L.F., Aluminum Alloys: Structure and Properties, pp. 311-323, Butterworths, 1976.
8. Wadsworth, J., Pelton, A.R., and Lewis, R.E., "Superplastic Al-Cu-Li-Mg-Zr Alloys," Metallurgical Transactions A, V. 16A, pp. 2319-2332, December 1985.
9. Sherby, O.D., and Ruano, O.A., "Synthesis and Characteristics of Superplastic Alloys," Superplastic Forming of Structural Alloys, Conference Proceedings of TMS-AIME and ASM 1982, N.E. Paton and C.H. Hamilton, eds., pp. 241-254, The Metallurgical Society of AIME, 1982.
10. Hales, S.J. and McNelley, T.R., "Microstructural Evolution by Continuous Recrystallization in a Superplastic Al-Mg Alloy," submitted to Acta Metallurgica, unpublished research, Naval Postgraduate School, Monterey, California, January 1987.
11. Stowell, M.J., "Cavitation in Superplasticity," Superplastic Forming of Structural Alloys, Conference Proceedings of TMS-AIME and ASM 1982, N.E. Paton and C.H. Hamilton, eds., pp. 321-336, The Metallurgical Society of AIME, 1982.

12. Lloyd, D.J., and Moore, D.M., "Aluminum Alloy Design for Superplasticity," Superplastic Forming of Structural Alloys, Conference Proceedings of TMS-AIME and ASM 1982, N.E. Paton and C.H. Hamilton, eds., pp. 147-169, The Metallurgical Society of AIME, 1982.
13. Sherby, O.D. and Wadsworth, J., "Development and Characterization of Fine-Grain Superplastic Materials," Deformation, Processing, and Structure, Papers presented at the 1982 ASM Materials Science Seminar, pp. 355-388, American Society for Metals, 1984.
14. Smallman, R.E., Modern Physical Metallurgy, 4th Ed., pp. 363-366, Butterworths, 1985.
15. Hull, D., Introduction to Dislocations, 2nd Ed., pp. 192-224, Pergamon Press, 1975.
16. Wert, J.A., "Thermomechanical Processing of Heat Treatable Aluminum Alloys for Grain Size Control," Microstructural Control in Aluminum Alloys, pp. 66-94, The Metallurgical Society, Inc., 1986.
17. Nes, E., "Strain-Induced Continuous Recrystallization in Zr-bearing Aluminum Alloys," Journal of Materials Science, V. 13, pp. 2052-2055, 1978.
18. Ahlborn, H., Hornbogen, E., and Koster, V., "Recrystallization Mechanism and Annealing Texture in Aluminum-Copper Alloys," Journal of Material Science, V. 4, pp. 944-950, 1969.
19. Watts, B.M., Stowell, M.J., Baike, B.L. and Owen, D.G.E., "Superplasticity in Al-Cu-Zr Alloys, Part I: Material Preparation and Properties," Metal Science, V. 10, pp. 189-197, June 1976.
20. Watts, B.M., Stowell, M.J., Baike, B.L., and Owen, D.G.E., "Superplasticity in Al-Cu-Zr Alloys, Part II: Microstructural Study," Metal Science, V. 10, pp. 198-206, June 1976.
21. Berthold, D.B., Effect of Temperature and Strain Rate on Microstructure of a Deformed, Superplastic Al-10%Mg-0.1%Zr Alloy, Master's Thesis, Naval Postgraduate School, Monterey, California, June 1985.
22. Alcamo, M.E., Effect of Strain Rate on the Microstructure of a Superplastically Deformed Al-10%Mg-0.1%Zr Alloy, Master's Thesis, Naval Postgraduate School, Monterey, California, June 1985.

23. Klankowski, K.A., Retrained Ambient Temperature Properties of Superplastically Deformed Al-10%Mg-0.1%Zr, Al-10%Mg-0.5%Mn, Al-10%Mg-0.4%Cu Alloys, Master's Thesis, Naval Postgraduate School, Monterey, California, December 1985.
24. Hartmann, T.S., Mechanical Characteristics of a Superplastic Aluminum--10.2%Mg-0.1%Zr Alloy, Master's Thesis, Naval Postgraduate School, Monterey, California, June 1985.
25. Grider, W.J., The Effect of Thermomechanical Processing Variables on Ductility of a High-Mg, Al-Mg-Zr Alloy, Master's Thesis, Naval Postgraduate School, Monterey, California, June 1986.
26. Solomos, D., The Effect of Processing and Superplastic Deformation on Ambient Ductility of Al-Mg-Zr Alloy, Master's Thesis, Naval Postgraduate School, Monterey, California, March 1987.
27. Andrews, J.N., A Calorimetric Study of the Microstructures of a Thermomechanically Processed Al-10%Mg-0.1%Zr Alloy, Master's Thesis, Naval Postgraduate School, Monterey, California, September 1986.
28. Wise, J.E., The Influence of Total Strain, Strain Rate, and Reheating Time During Warm Rolling on the Superplastic Ductility of an Al-Mg-Zr Alloy, Master's Thesis, Naval Postgraduate School, Monterey, California, March 1987.
29. Howe, J.M., "Metallographic and Differential Scanning Calorimetry of Precipitation and Recrystallization in an Al-Mn Alloy," Metallurgical Transactions A, V. 17A, pp. 363-604, April 1986.
30. Lendvai, J., Honyek, G., and Kovacs, I., "Dissolution of Second Phases in Al-Zn-Mg Alloy Investigated by Calorimetric Method," Scripta Metallurgica, V. 13, pp. 393-394, 1979.
31. DeLasi, R. and Adler, P.N., "Calorimetric Studies of 7000 Series Alloys: I. Matrix Precipitate Characterization of 7075," Metallurgical Transactions A, V. 8A, pp. 1177-1183, July 1977.
32. Papazian, J.M., "Calorimetric Studies of Precipitation and Dissolution Kinetics in Aluminum Alloys 2219 and 7075," Metallurgical Transactions A, V. 13A, pp. 761-769, May 1982.

33. McNaughton, J.L. and Mortimer, C.T., "Differential Scanning Calorimetry," IRS: Physical Chemistry Series 2, V. 10, Butterworths, 1975, reprinted with permission by Perkin-Elmer Corporation.
34. Adler, P.N. and DeIasi, R., "Calorimetric Studies of 7000 Series Alloys: II. Comparison of 7075, 7050, and RX720 Alloys," Metallurgical Transactions A, V. 8A, pp. 1185-1190, July 1977.
35. Lacom, W., Degischer, H.P., Azhra, A.M., and Zahra, C.Y., "On Calorimetric and Electron Microscopic Studies of Al-Zn-Mg Alloys," Scripta Metallurgica, V. 14, pp. 253-254, 1980.
36. AlCOA Technical Center, letter, 20 August 1984.
37. Johnson, R.B., The Influence of Alloy Composition and Thermomechanical Processing Procedure on Microstructural and Mechanical Properties of High-Magnesium Aluminum Alloys, Master's Thesis, Naval Postgraduate School, Monterey, California, June 1980.
38. Becker, J.J., Superplasticity in Thermomechanically Processed High-Magnesium Aluminum Magnesium Alloys, Master's Thesis, Naval Postgraduate School, Monterey, California, March 1984.
39. Lee, Eo-Wo and McNelley, T.R., "Application of a Thermo-mechanical Process for Grain Refinement of Al-7475," submitted to Material Science and Engineering, unpublished research, Naval Postgraduate School, Monterey, California, 1986.

INITIAL DISTRIBUTION LIST

	No. Copies
1. Defense Technical Information Center Cameron Station Alexandria, Virginia 22304-6145	2
2. Library, Code 0142 Naval Postgraduate School Monterey, California 93943-5002	2
3. Department Chairman, Code 69Hy Department of Mechanical Engineering Naval Postgraduate School Monterey, California 93943-5000	1
4. Professor T.R. McNelley, Code 69Mc Department of Mechanical Engineering Naval Postgraduate School Monterey, California 93943-5000	5
5. Dr. S.J. Hales, Code 69Ha Department of Mechanical Engineering Naval Postgraduate School Monterey, California 93943-5000	1
6. Professor A.J. Perkins, Code 69Ps Department of Mechanical Engineering Naval Postgraduate School Monterey, California 93943-5000	1
7. Naval Air Systems Command, Code AIR 931 Attn: L. Slotter Naval Air Systems Command Headquarters Washington, D.C. 20361	1
8. Dr. Jeffrey Waldman, Code 606 Naval Air Development Center Warminster, Pennsylvania 19874	1
9. Dr. Eui-Whee Lee, Code 6063 Naval Air Development Center Warminster, Pennsylvania 19874	1
10. LCDR J.N. Andrews, USN Supervisor of Shipbuilding, Conversion, and Repair Pascagoula, Mississippi 39567	1

11. LCDR Donald L. Stewart, USN
515 Harolds Drive
Huntsville, Alabama 35806

8

END

11-87

DTIC